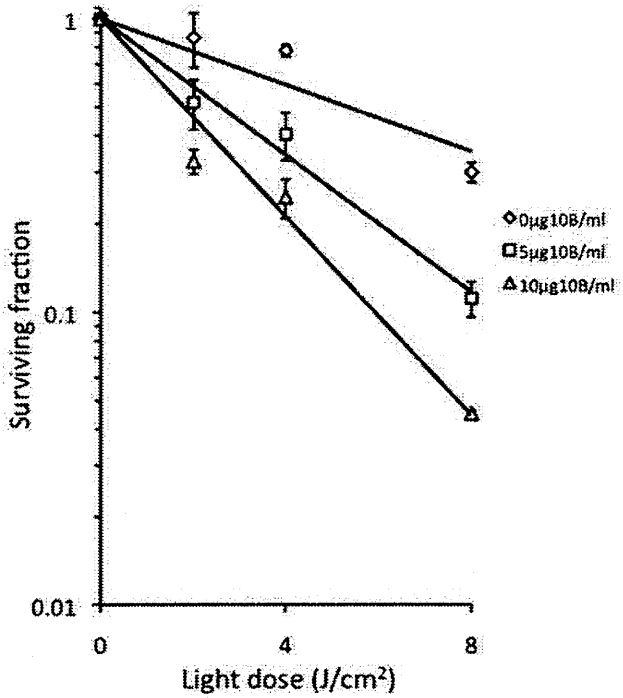

Fig. 3. Colony-forming assay using F98 rat glioma cells exposed to 0 (control), 5, and 10 μg B/ml of H_2OCP and irradiated with light doses of 0, 2, 4, and 8 J/cm^2, respectively. The cell-surviving fraction following laser irradiation (8 J/cm^2, 18 hours after exposure to 10 μg B/ml H_2OCP) was <0.05.

Tumorigenesis of In Vitro Pre-Treated Tumor Cells

The observed tumorigenicity of the implanted pre-treated cells using Kaplan–Meier survival curves revealed median survival times of 12 and 14 days in the untreated and the treated groups, respectively, and mean survival times of 11.8 and 14.6 days after implantation, respectively. In Kaplan–Meier survival curve analysis, these survival times demonstrated a significant difference (log-rank test, $P < 0.05$) (Fig. 4).

Cytotoxicity of H_2OCP in Dark Conditions

The viable cell-counting method revealed the following results. The percentage of cell viability with exposure of 20 μg B/ml H_2OCP was 98.0 ± 1.4% (mean ± SD), while that of cell viability without H_2OCP was 98.0 ± 0.9%. The colony-forming assay showed the following: the surviving fractions with each boron concentration (0, 5, 10, 20, 40 μg B/ml H_2OCP) were 1, 0.99 ± 0.04 (mean ± SD), 0.98 ± 0.05, 0.98 ± 0.01, and 0.98 ± 0.03, respectively. These results showed no significant differences (Welch's t-test, $P > 0.05$).

Fluorescence Microscopy

The fluorescence microscopy showed the intracellular porphyrin fluorescence and images from the co-localization

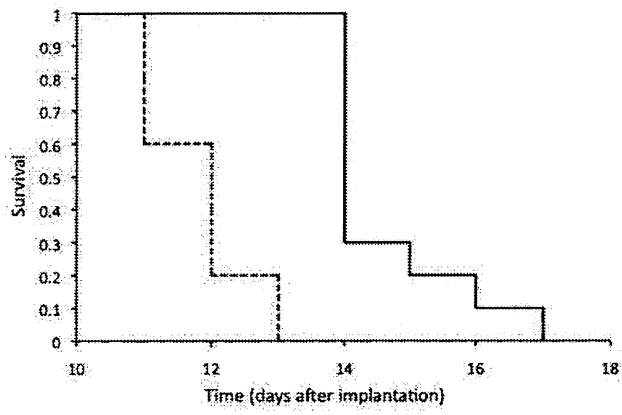

Fig. 4. Kaplan–Meier survival curves following in vitro pre-treated F98 cells using H_2OCP-mediated PDT. Rats were implanted i.c. with F98 cells and were either untreated (dotted line) or treated with PDT (continuous line). Cells were exposed to 20 μg B/ml of H_2OCP for 24 hours at 37°C prior to laser irradiation. After laser irradiation (4 J/cm^2), the tumor cells were implanted into the rats. Cell viability was determined by trypan blue exclusion staining and 10^5 viable cells were implanted stereotactically into the caudate nucleus. The median survival times of the untreated control and the treated group were 12 and 14 days, and the mean survival times were 11.8 and 14.6 days after implantation, respectively ($P < 0.05$).

experiment using the nucleus-specific Hoechst dye. These results showed that H_2OCP was taken up into the cells and also localized in the nuclei (Fig. 5B–D). Although the cells showed evidence of cytotoxic damage, the cytotoxicity of H_2OCP in dark conditions was not found at twice the concentration of H_2OCP used in this fluorescence microscopy experiment. (Fig. 5A).

DISCUSSION

BNCT is a targeted chemo-radiation therapy that significantly increases the therapeutic ratio relative to conventional radiotherapeutic modalities. In BNCT, a ^{10}B-labeled compound delivers therapeutic concentrations of ^{10}B (~30 μg ^{10}B/g tumor) to the target tumor, with high tumor-to-blood and tumor-to-normal-tissue ratios and low cytotoxicity [5,6]. Subsequently the tumor is irradiated with epithermal neutrons that become thermalized at a certain depth within the tissues. The short range (<10 μm) of the α and ^{7}Li high linear energy transfer (high-LET) particles released from the ^{10}B(n, α) ^{7}Li neutron capture reaction makes the tumor microdistribution of ^{10}B critically important in BNCT [21]. Since the high-LET particles are highly cytotoxic, their killing effect depends on the site of generation. These characteristics contribute to the tumor selectivity and strong tumoricidal activity of BNCT, with negligible damage to normal tissue. Therefore, if sufficient quantities of boron can be selectively delivered to tumor tissues, BNCT could be an ideal tumor-selective particle

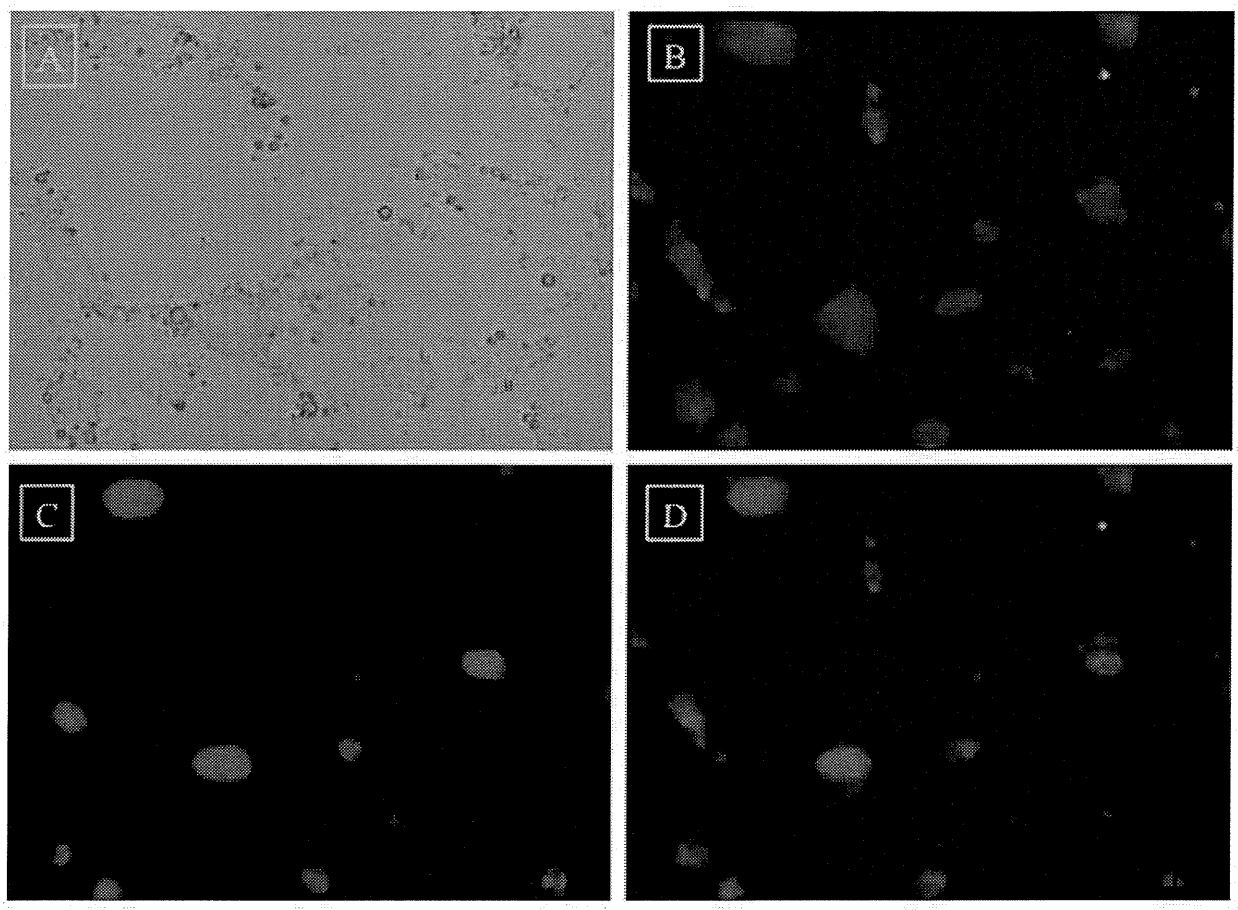

Fig. 5. Images obtained using an inverted fluorescence microscope. **A**: Bright field image. Although the cells showed evidence of cytotoxic damage, the cytotoxicity of H_2OCP in dark conditions was not found at twice the concentration of H_2OCP used in this fluorescence microscopy experiment. **B**: Fluorescence of porphyrin H_2OCP. **C**: Nuclear fluorescence by Hoechst dye (excitation wavelength was 340–380 nm). **D**: Merged image. (Magnification of all images: ×600).

beam irradiation local therapy for malignant gliomas. Clinically, BPA and BSH are currently available for BNCT as boron delivery agents. BPA is a boronated derivative of an essential amino acid (L-phenylalanine) that is actively taken up by tumor cells, presumably via the amino acid transport mechanism [22]. BSH, on the other hand, is believed to preferentially accumulate within tumor tissue via a partially destroyed or leaky blood brain barrier, and is thought to be retained longer than BPA due to its higher hydrophobic character [23]. We have used both of these boron delivery agents in combination in clinical BNCT studies, and have previously been reported on the survival benefit from BNCT for newly diagnosed GB patients [7] as well as for recurrent malignant glioma patients [8]. However, the present results using BPA and BSH are far from satisfactory, and the use of more effective boron delivery agents should provide enhanced clinical outcomes for BNCT. The so-called third-generation of boron delivery agents [6], including boronated porphyrin derivatives, molecular-targeted agents (e.g., to EGFR), and liposome-linked boron delivery agents could potentially greatly increase the efficacy of BNCT in the clinical setting. Among these boron delivery agents, boronated porphyrins are particularly promising because they contain a porphyrin ring with tumor affinity, and they are also excellent photosensitizers for PDT [9]. In a similar fashion to BNCT, PDT is a localized therapy that relies on the specific uptake of a photosensitizer in the tumor relative to the surrounding normal tissue, followed by laser irradiation for activation of the photosensitizer [2,24]. The photoactivation of the sensitizer causes oxidative damage to a variety of cellular targets via the release of singlet oxygen and other reactive oxygen species, with subsequent tumor necrosis. To date, the clinical trials with PDT employed as an adjuvant treatment for human gliomas have used the poorly defined heterogeneous porphyrin mixture hematoporphyrin derivative (HpD) or its more enriched

commercial preparation, Photofrin [2], which does not contain boron. This photosensitizer has been shown to localize preferentially in glioma relative to normal brain tissue. Moreover, reports of PDT as a treatment for animal and human glioma have been encouraging, and a photosensitizer that is more tumor selective than HpD or Photofrin would have great clinical benefits.

In this study, our results showed the positive efficacy of PDT using H_2OCP in a colony-forming assay (Fig. 3) and in tumorigenesis of in vitro pre-treated cells in Fisher rats (Fig. 4). Additionally, H_2OCP accumulated within the glioma cells to a significantly higher extent than BPA or BSH ($P < 0.05$), and was retained inside the cell to approximately the same extent as BSH (Fig. 2). Based on these findings, we postulated that H_2OCP could be applied to both PDT and BNCT for treatment of glioma tumors. In the fluorescence microscopy experiment, although the cells in the bright field image showed evidence of cytotoxic damage (Fig. 5A), the cytotoxicity of H_2OCP in dark conditions was not observed, even at double the concentration of H_2OCP used in the fluorescence microscopy experiment. Therefore, we considered that the damage to the cells in the bright field image was most probably due to technical complications related to irradiation with the laser during imaging, rather than to the cytotoxic effects of H_2OCP itself. Furthermore, H_2OCP was shown to be taken up by F98 rat glioma cells (Fig. 5B–D). Therefore, our results suggest that H_2OCP can be used intraoperatively for photodynamic diagnosis (PDD) and fluorescence-guided resection of brain tumors.

Pre-operative administration of a boronated porphyrin has a number of advantages in the clinical setting. As noted previously, boronated porphyrins are useful in PDD and in fluorescence-guided resection of brain tumors during surgery. Using fluorescence-guided resection of such tumors during surgery, the resection rate can be augmented, with expected further improvements in patient prognosis [25]. In addition, boronated porphyrins can be used with intra-operative PDT and post-operative BNCT. Although the initial results with commonly used photosensitizers for PDT such as Photofrin (or its unpurified form HpD) were very encouraging, treatment failures did occur, mainly due to the limited penetration of light into the brain. In cases with deep lesions, PDT alone may be inadequate to achieve complete tumor treatment, and it would be preferable in such cases to use BNCT as a supplementary treatment, with boron-containing porphyrin as a photosensitizer. Fairchild et al. [26] reported that thermal and epithermal neutrons are transported to a depth of approximately 10 cm in fact, BNCT has been shown to treat deep lesions. Since boronated porphyrins can be effective for BNCT as boron delivery agents while retaining their photosensitizer ability, the limited penetration of light can be overcome using a combination of BNCT and PDT for the treatment of human gliomas.

ACKNOWLEDGMENTS

This work was supported by Grants-in-Aid for Scientific Research (C) (20340549) from the Japanese Ministry of Education, Culture, Sports, Science, and Technology (MEXT) to SK and by the United States National Institutes of Health, grant number R01 CA 098902, to MGHV. We thank Dr. Barth (Department of Pathology, the Ohio State University) for providing the F98 rat glioma cells. Authorship standards: RH performed all in vitro/ex vivo studies; SK designed the experiments, interpreted data, supervised all in vitro studies, and reviewed the manuscript; SM reviewed the manuscript; TK reviewed the manuscript; MWE synthesized H_2OCP and reviewed the manuscript; MGHV synthesized H_2OCP, interpreted data, and reviewed the manuscript. All authors have read and approved the final manuscript.

REFERENCES

1. Stupp R, Hegi ME, van den Bent MJ, Mason WP, Weller M, Mirimanoff RO, Cairncross JG. Changing paradigms – An update on the multidisciplinary management of malignant glioma. Oncologist 2006;11(2):165–180.
2. Kaye AH, Hill JS. Photodynamic therapy of cerebral tumors. Neurosurg Q 1992;1:233–258.
3. Origitano TC, Caron MJ, Reichman OH. Photodynamic therapy for intracranial neoplasms. Literature review and institutional experience. Mol Chem Neuropathol 1994; 21(2–3):337–352.
4. Kostron H, Obwegeser A, Jakober R. Photodynamic therapy in neurosurgery: A review. J Photochem Photobiol B 1996;36(2): 157–168.
5. Barth RF, Soloway AH, Fairchild RG, Brugger RM. Boron neutron capture therapy for cancer. Realities and prospects. Cancer 1992;70(12):2995–3007.
6. Barth RF, Coderre JA, Vicente MG, Blue TE. Boron neutron capture therapy of cancer: Current status and future prospects. Clin Cancer Res 2005;11(11):3987–4002.
7. Kawabata S, Miyatake S, Kuroiwa T, Yokoyama K, Doi A, Iida K, Miyata S, Nonoguchi N, Michiue H, Takahashi M, Inomata T, Imahori Y, Kirihata M, Sakurai Y, Maruhashi A, Kumada H, Ono K. Boron neutron capture therapy for newly diagnosed glioblastoma. J Radiat Res (Tokyo) 2009;50(1):51–60.
8. Miyatake S, Kawabata S, Yokoyama K, Kuroiwa T, Michiue H, Sakurai Y, Kumada H, Suzuki M, Maruhashi A, Kirihata M, Ono K. Survival benefit of boron neutron capture therapy for recurrent malignant gliomas. J Neurooncol 2009;91(2):199–206.
9. Vicente MGH, Sibrian-Vazquez M. Syntheses of boronated porphyrins and their application in BNCT. In: Kadish KM, Smith KM, Guilard R, eds. The Handbook of Porphyrin Science. Vol. 4. Singapore: World Scientific Publishers; 2010: 191–248.
10. Renner MW, Miura M, Easson MW, Vicente MGH. Recent progress in the syntheses and biological evaluation of boronated porphyrins for boron neutron-capture therapy. Anticancer Agents Med Chem 2006;6(2):145–157.
11. Ceberg CP, Brun A, Kahl SB, Koo MS, Persson BR, Salford LG. A comparative study on the pharmacokinetics and biodistribution of boronated porphyrin (BOPP) and sulfhydryl boron hydride (BSH) in the RG2 rat glioma model. J Neurosurg 1995;83(1):86–92.
12. Ozawa T, Afzal J, Lamborn KR, Bollen AW, Bauer WF, Koo MS, Kahl SB, Deen DF. Toxicity, biodistribution, and convection-enhanced delivery of the boronated porphyrin BOPP in the 9L intracerebral rat glioma model. Int J Radiat Oncol Biol Phys 2005;63(1):247–252.
13. Miura M, Morris GM, Micca PL, Nawrocky MM, Makar MS, Cook SP, Slatkin DN. Synthesis of copper octabromotetracarboranylphenylporphyrin for boron neutron capture therapy and its toxicity and biodistribution in tumour-bearing mice. Br J Radiol 2004;77(919):573–580.
14. Hao E, Sibrian-Vazquez M, Serem W, Garno JC, Fronczek FR, Vicente MG. Synthesis, aggregation and cellular investigations of porphyrin-cobaltacarborane conjugates. Chemistry 2007;13(32):9035–9042.

15. Gottumukkala V, Luguya R, Fronczek FR, Vicente MG. Synthesis and cellular studies of an octa-anionic 5,10,15,20-tetra[3,5-(nido-carboranylmethyl)phenyl]porphyrin (H(2)OCP) for application in BNCT. Bioorg Med Chem 2005; 13(5):1633–1640.
16. Friso E, Roncucci G, Dei D, Soncin M, Fabris C, Chiti G, Colautti P, Esposito J, De Nardo L, Riccardo Rossi C, Nitti D, Giuntini F, Borsetto L, Jori G. A novel 10B-enriched carboranyl-containing phthalocyanine as a radio- and photo-sensitizing agent for boron neutron capture therapy and photodynamic therapy of tumours: In vitro and in vivo studies. Photochem Photobiol Sci 2006;5(1):39–50.
17. Coderre JA, Button TM, Mica PL, Fisher CD, Nawrocky MM, Liu HB. Neutron capture therapy of the 9L rat gliosarcoma using the p-boronophenylalanine-fructose complex. Int J Radiat Oncol Biol Phys 1994;30(3):643–652.
18. Barth RF. Rat brain tumor models in experimental neuro-oncology: The 9L, C6, T9, RG2 (D74), RT-2 and CNS-1 gliomas. J Neurooncol 1998;36(1):91–120.
19. Biston MC, Joubert A, Adam JF, Elleaume H, Bohic S, Charvet AM, Estève F, Foray N, Balosso J. Cure of Fisher rats bearing radioresistant F98 glioma treated with cis-platinum and irradiated with monochromatic synchrotron X-rays. Cancer Res 2004;64(7):2317–2323.
20. Kobayashi N, Allen N, Clendenon NR, Ko LW. An improved rat brain-tumor model. J Neurosurg 1980;53(6):808–815.
21. Taylor HJ, Goldhaber M. Detection of nuclear disintegration in a photographic emulsion. Nature 1935;135:341–341.
22. Snyder HR, Reedy AJ, Lennarz WJ. Synthesis of aromatic boronic acids. Aldehydo boronic acids and a boronic acid analog of tyrosine. J Am Chem Soc 1958;80:835–838.
23. Soloway AH, Hatanaka H, Davis MA. Penetration of brain and brain tumor: VII. Tumor-binding sulfhydryl boron compounds. J Med Chem 1967;10(4):714–717.
24. Dougherty TJ, Gomer CJ, Henderson BW, Jori G, Kessel D, Korbelik M, Moan J, Peng Q. Photodynamic therapy. J Natl Cancer Inst 1998;90(12):889–905.
25. Stummer W, Novotny A, Stepp H, Goetz C, Bise K, Reulen HJ. Fluorescence-guided resection of glioblastoma multiforme by using 5-aminolevulinic acid-induced porphyrins: A prospective study in 52 consecutive patients. J Neurosurg 2000;93(6): 1003–1013.
26. Fairchild RG, Saraf SK, Kalef-Ezra J, Laster BH. Comparison of measured parameters from a 24-keV and a broad spectrum epithermal neutron beam for neutron capture therapy: An identification of consequential parameters. Med Phys 1990; 17(6):1045–1052.

Computed Tomography Imaging of Transferrin Targeting Liposomes Encapsulating Both Boron and Iodine Contrast Agents by Convection-Enhanced Delivery to F98 Rat Glioma for Boron Neutron Capture Therapy

Shiro Miyata, MD*
Shinji Kawabata, MD, PhD*
Ryo Hiramatsu, MD*
Atsushi Doi, MD, PhD*
Naokado Ikeda, MD, PhD*
Taro Yamashita, MD*
Toshihiko Kuroiwa, MD, PhD*
Satoshi Kasaoka, PhD‡
Kazuo Maruyama, PhD§
Shin-Ichi Miyatake, MD, PhD*

*Department of Neurosurgery, Osaka Medical College, Osaka, Japan; ‡Faculty of Pharmaceutical Sciences, Hiroshima International University, Hiroshima, Japan; §Faculty of Pharmaceutical Sciences, Teikyo University, Tokyo, Japan.

Correspondence:
Shinji Kawabata, MD, PhD,
Department of Neurosurgery,
Osaka Medical College,
2-7 Daigaku-machi,
Takatsuki City,
Osaka 569-8686, Japan.
E-mail: neu046@poh.osaka-med.ac.jp.

Received, February 4, 2010.
Accepted, October 2, 2010.

BACKGROUND: To achieve potent tumor-selective antitumor efficacy by boron neutron capture therapy (BNCT), it is important to have a significant differential uptake of ^{10}B between tumor cells and normal cells. This should enable BNCT to reduce damage to normal tissues compared with other radiation therapies.

OBJECTIVE: To augment the therapeutic efficacy of BNCT, we used transferrin-conjugated polyethylene glycol (PEG) (TF-PEG) liposome encapsulating sodium borocaptate and lomeprol, an iodine contrast agent, with intratumoral convection-enhanced delivery (CED) in a rat glioma tumor model.

METHODS: The in vitro ^{10}B concentration of F98 rat glioma cells was determined by inductively coupled plasma atomic emission spectrometry after incubation with either TF-PEG or PEG liposomes. For in vivo biodistribution studies, ^{10}B concentrations within blood, normal brain tissue, and intracerebrally transplanted F98 cells were measured with inductively coupled plasma-atomic emission spectrometry after CED of the compounds, and computed tomography was performed at selected time intervals.

RESULTS: ^{10}B concentrations of F98 cultured glioma cells in vitro 6 hours after exposure to PEG and TF-PEG liposome were 16.1 and 51.9 ng $^{10}B/10^6$ cells, respectively. ^{10}B concentrations in F98 glioma tissue 24 hours after CED were 22.5 and 82.2 μg/g, by PEG and TF-PEG liposome, respectively, with lower ^{10}B concentrations in blood and normal brain. Iomeprol provided vivid and stable enhanced computed tomography imaging of the transplanted tumor even 72 hours after CED by TF-PEG liposome. Conversely, tissue enhancement had already washed out at 24 hours after CED of the PEG liposomes.

CONCLUSION: The combination of TF-PEG liposome encapsulating sodium borocaptate and lomeprol and intratumoral CED enables not only a precise and potent targeting of boron delivery to the tumor tissue, but also the ability to follow the trace of boron delivery administered intratumorally by real-time computed tomography.

KEY WORDS: Boron neutron capture therapy, Computed tomography, Convection-enhanced delivery, Liposome, Transferrin

Neurosurgery 68:1380–1387, 2011 DOI: 10.1227/NEU.0b013e31820bb52aa www.neurosurgery-online.com

ABBREVIATIONS: ^{10}B, boron-10; **BBB**, blood-brain barrier; **BDS**, boron delivery system; **BNCT**, boron neutron capture therapy; **BSH**, sodium borocaptate; **CED**, convection-enhanced delivery; **PEG**, polyethylene glycol; **TF-PEG**, transferrin-conjugated polyethylene glycol

Supplemental digital content is available for this article. Direct URL citations appear in the printed text and are provided in the HTML and PDF versions of this article on the journal's Web site (www.neurosurgery-online.com).

Therapeutic modalities such as stereotactic radiosurgery, intensity-modulated radiation therapy, particle radiation therapy, and novel therapeutic agents with molecular targeting have been developed to improve the prognosis of some types of brain tumors. However, over the past few decades, there has been little improvement in the prognosis of

patients with malignant gliomas because of the tumor's tendency to microscopically infiltrate the surrounding normal tissue. To overcome this infiltrative nature, it is necessary to selectively deliver a higher concentration of anticancer or radiation sensitizing agents into tumor tissue compared with the surrounding normal brain tissue. We are focusing on developing boron neutron capture therapy (BNCT) to achieve greater tumor-selective killing and therefore therapeutic efficacy.

At our institution, we have clinically applied BNCT since 2002 as an essential adjuvant therapy for patients with recurrent or newly diagnosed malignant gliomas[1-4] and have achieved superior outcomes compared with those by standard therapies using fractionated radiographic treatments.[5] BNCT is based on the nuclear capture and fission reactions that occur when boron-10 (^{10}B), a nonradioactive constituent of natural elemental boron, is irradiated with low-energy thermal neutrons to produce high-energy α particles and recoiling lithium-7 nuclei. These have high linear energy transfer and path lengths of approximately 9 and 5 μm, respectively, which theoretically allow them to discharge their energy within ^{10}B-containing cells.[6] Thus, to achieve potent tumor-selective antitumor efficacy, it is important to have a significant differential uptake of ^{10}B between tumor cells and normal cells. This should enable BNCT to reduce damage to normal tissues compared with other radiation therapies.

Today, clinically used sodium borocaptate (BSH) is transferred to brain tumors only through the disrupted blood-brain barrier (BBB), so it is difficult for BSH to reach regions that tumor cells invade microscopically where the BBB seems to be intact. On the other hand, boronophenylalanine, which transfers boron via L-type amino acid transporter, can deliver ^{10}B even in the infiltrating tumor cell population where the BBB is intact. However, some amounts of ^{10}B are inevitably taken into the normal cells by boronophenylalanine systemic administration. Moreover, the native heterogeneity of malignant gliomas interferes with the ability to accurately target the tumor. Recent reports have delineated boron delivery systems (BDSs) to improve molecular targeting of malignant gliomas.[7,8] Previously we reported on the effectiveness of transferrin-conjugated polyethylene glycol (PEG) (TF-PEG) liposome encapsulating BSH administered intravenously, with regard to its ability to target tumor cells and to increase the accumulation of ^{10}B in tumor tissue.[9]

To improve the efficacy of tumor targeting under systemic administration, the circulation time of a BDS in the blood needs to be lengthened. Unfortunately, systemic administration of a BDS increases the capture of ^{10}B-labeled molecules in the reticuloendothelial system of the liver and spleen, which may cause adverse effects. To solve these problems, we adopted convection-enhanced delivery (CED) for drug administration. This technique enables the delivery of boron compounds to the tumor cells in the brain without going through the disrupted BBB. CED, a method for local drug infusion directly into the brain,[10] enables the distribution of any drugs homogeneously in the brain, keeping high concentration at the target site without mechanical damage to the surrounding normal tissue. CED depends on the bulk flow in the interstitial space produced by continuous slow infusion into the brain under low positive pressure. Using this method, it is theoretically possible to deliver drugs to regions where tumor cells invade microscopically with little accumulation in the blood and other organs. Moreover, because it does not depend on the molecular weight of the infused agent, this method allows us to widely select many kinds of therapeutic agents or carriers for them, such as liposomes, dendrimers, and nanotubes.[7,11-15] Today, some clinical trials of targeted toxins with epidermal growth factor receptor, transferrin receptor, interleukin-13 receptor, and interleukin-4 receptor are reported.[8,11,16-18]

In BNCT, there is some interval before neutron irradiation, unlike with chemotherapies or therapies by toxins. This interval derives from the nontoxicity of BDS, and it enables us to estimate the distribution of infusion agents before neutron irradiation. We developed a novel liposomal BDS mechanism that encapsulates BSH and an iodine contrast agent, making it possible to trace the intracerebral distribution of the drug by computed tomography (CT).[19] We evaluated 2 BDSs: PEG liposome encapsulating both BSH and Iomeprol (PEG liposome [BSH, Iomeprol]) and TF-PEG liposome (BSH, Iomeprol) administered by CED in rat brain tumor models.

MATERIALS AND METHODS

Preparation of the Boron Compounds

BSH was purchased from Katchem (Prague, Czech Republic). Iomeprol was used as an iodine contrast agent for CT scanning. Iomeprol (MW777.09, concentration 612.4 mg/mL; Iomeron 300; Eisai, Tokyo, Japan), which is very soluble in water and contains 300 mg/mL organically bound iodine, was used as the imaging tracer. PEG liposome (BSH, Iomeprol) and TF-PEG liposome (BSH, Iomeprol) were prepared by one of the authors (S.K.) as reported previously.[20] Transferrin (1:60 transferrin:phospholipid molar ratio; phospholipid concentration, 0.2 mM) (Wako Pure Chemical Industries, Osaka, Japan) was conjugated to the distal ends of 1,2-dioleoyl-sn-glycero-3-phosphoethanolamine-n-[poly(ethyleneglycol)]-hydroxy succinamide (Nippon Oil and Fats, Tokyo, Japan) in micelles at room temperature for 1 hour with gentle stirring. TF-PEG distearoylphosphatidylethanolamine (DSPE) was transferred to preformed PEG liposomes (64:33:3 dipalmitoylphosphatidylcholine (DPPC):cholesterol:DSPE-PEG molar ratio; size <150 nm) loaded with 300 mM BSH:Iomeprol at a 1:1 volume ratio using the micelle transfer method at a 1:33 TF-PEG-DSPE:liposome molar ratio, at 45°C for 3 hours. Both PEG liposome (BSH, Iomeprol) and TF-PEG liposome (BSH, Iomeprol) were prepared using the protocol described by Wei et al[7] with slight modifications.

To evaluate possible adverse effects of PEG liposome (BSH, Iomeprol) and TF-PEG liposome (BSH, Iomeprol) on normal brain parenchyma, 12 Fischer 344 male rats (200-230 g, F344 NSlc; Japan SLC, Shizuoka, Japan) were given a 20-μg ^{10}B infusion of either BDS (n = 6 per BDS) into the right hemisphere by CED. Body weight was measured just before the CED procedure and on days 7 and 14 after the procedure. Some of the rats that were administered either BDS were euthanized on day 7 after the CED procedure for histological evaluation and were perfused with 4% paraformaldehyde; their brains were then processed for histological examination with hematoxylin and eosin staining.

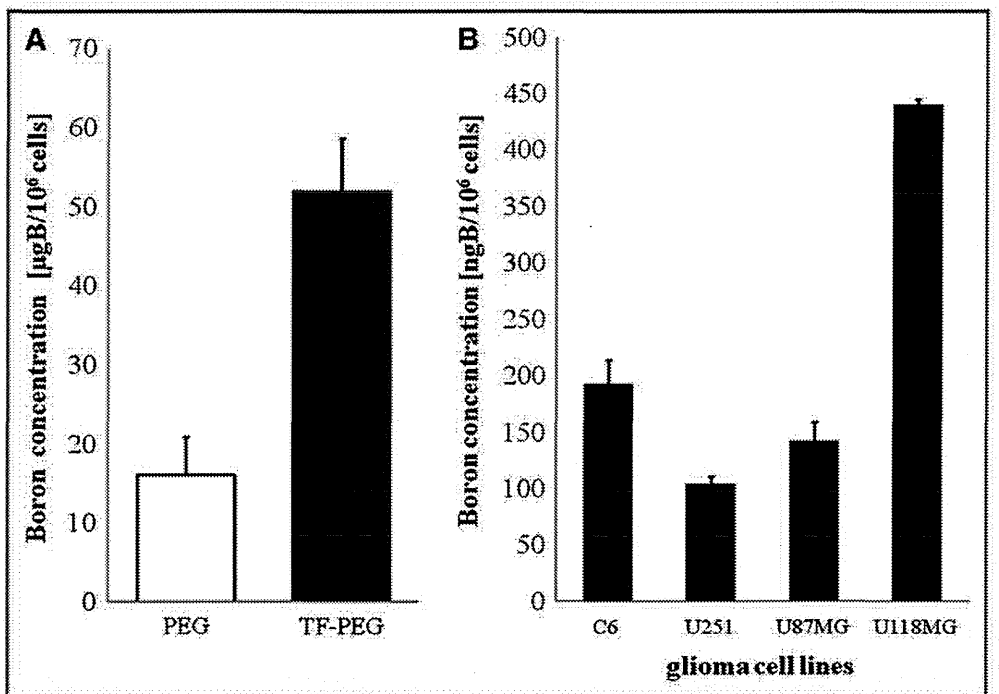

FIGURE 1. *A, boron concentration of F98 glioma cells 6 hours after incubation in media including 10 μg ^{10}B/mL of each boron delivery system. Transferrin-conjugated polyethylene glycol (TF-PEG) group (■) and the polyethylene glycol (PEG) group (□). The boron concentrations of tumor cells were significantly higher in the TF-PEG group than in the PEG group: 51.9 ± 6.8 ng ^{10}B/10^6 cells and 16.1 ± 4.8 ng ^{10}B/10^6 cells, respectively (P < .05). B, boron concentration of glioma cells (C6, U251, U87MG, and U118MG) 6 hours after incubation for 10 μg ^{10}B/mL of TF-PEG liposome. F98 glioma cells showed the minimum accumulation of sodium borocaptate by this liposome among these glioma cell lines.*

In Vitro Cellular Uptake Study

For the in vitro boron uptake study, F98 rat glioma cells (provided by Rolf F. Barth MD, The Ohio State University, Columbus, Ohio) were used. One million F98 glioma cells were seeded onto a tissue culture dish (100 × 20 mm; Becton Dickinson, Franklin Lakes, New Jersey) with Dulbecco modified Eagle medium with 10% fetal bovine serum with penicillin and streptomycin at 37°C in an atmosphere of 5% CO_2. All the materials for the culture medium were purchased from Invitrogen (Carlsbad, California). After incubation for 24 hours at 37°C, the medium was replaced with Dulbecco modified Eagle medium containing 10 μg ^{10}B/mL PEG liposome (BSH, Iomeprol) or TF-PEG liposome (BSH, Iomeprol), and the cells were incubated for an additional 6 hours at 37°C. The medium was then removed, and the cells were washed twice with phosphate-buffered saline and detached with trypsin–ethylenediamine tetraacetic acid solution. Medium was then added, and the cells were counted and sedimented. Cells were digested overnight with 1 N nitric acid solution (Wako Pure Chemical Industries), and boron uptake was determined by inductively coupled plasma-atomic emission spectrometry (Hitachi, Tokyo, Japan). Cellular uptake of boron by TF-PEG liposome (BSH, Iomeprol) for other glioma cell lines (C6, U251, U87MG, and U118MG) was also evaluated.

Tumor Model

The male Fischer 344 rats were generally anesthetized with an intraperitoneal injection of pentobarbital sodium (50 mg/kg) and placed in a stereotactic frame (Model 900; David Kopf Instruments, Tujunga, California). A midline incision was made in the scalp, and the skull target (3.5 mm right to the bregma) was identified. A hand-held drill was used to create a small burr hole at this location. A 25 μL Hamilton infusion syringe (model 1700 RN, Hamilton Bonaduz AG, Bonaduz, Switzerland) was fixed on the clamping device of the stereotactic frame. A 26-gauge needle attached to a microsyringe was first inserted to a depth of 6.0 mm from the skull and then withdrawn to its target depth in the brain (5.5 mm from the skull surface). Ten thousand F98 cells diluted in 10 μL of Dulbecco modified Eagle medium were then injected over approximately 10 minutes. The needle was kept in place for 1 minute after infusion and withdrawn slowly. The skull hole was sealed with bone wax, and the scalp was sutured. Under these conditions, the procedure results in tumor growth in all rats, with a median survival time of 23 days.

In Vivo Biodistribution Study

For biodistribution study, 10 days after tumor implantation, rats bearing F98 brain tumors were generally anesthetized and placed in a stereotactic frame as described above. They were administered either PEG liposome (BSH, Iomeprol) or TF-PEG liposome (BSH, Iomeprol) by CED with an infusion syringe pump over 30 minutes at a rate of 0.33 μL/min. The total amount of ^{10}B administered to each rat was 20 μg. We then assayed the ^{10}B concentration of tumor, blood, and normal brain by inductively coupled plasma-atomic emission spectrometry. In this study, we sampled normal tissues from both

TABLE 1. Boron Concentrations in Brain Tumors in Rats Bearing F98 Gliomas to Which Polyethylene Glycol Liposome (Sodium Borocaptate, Iomeprol) or Transferrin-Conjugated Polyethylene Glycol Liposome (Sodium Borocaptate), Iomeprol) Was Administered by Convection-Enhanced Delivery[a]

		Boron Concentration, μg/g				Tumor Brain Ratio	
BDS	Time, h[b]	Tumor	Brain Ipsilateral	Brain Contralateral	Blood	Ipsilateral Normal Brain	Contralateral Normal Brain
PEG liposome (BSH, Iomeprol)	0[c]	33.5 ± 10.5	0.6 ± 0.6	0.3 ± 0.1	0.4 ± 0.2	55.8	111.7
	24	22.5 ± 6.1	1.7 ± 1.5	1.0 ± 0.6	0.4 ± 0.1	13.2	22.5
	48	8.5 ± 7.9	1.5 ± 0.7	0.4 ± 0.3	0.4 ± 0.1	5.7	21.3
	72	4.9 ± 4.6	0.2 ± 0.1	0.2 ± 0.1	0.5 ± 0.2	24.5	24.5
TF-PEG liposome (BSH, Iomeprol)	0	55.2 ± 26.6	2.1 ± 2.5	0.4 ± 0.2	0.6 ± 0.3	26.3	138.0
	24	82.2 ± 18.6	0.7 ± 0.4	0.3 ± 0.2	0.6 ± 0.1	117.0	274.0
	48	41.2 ± 14.4	1.2 ± 1.0	0.9 ± 0.6	0.9 ± 0.1	34.3	45.8
	72	25.8 ± 13.5	0.4 ± 0.2	0.4 ± 0.2	0.6 ± 0.2	64.5	64.5

[a]Each point represents the mean ± standard deviation. BDS, boron delivery system; PEG, polyethylene glycol; BSH, sodium borocaptate; TF-PEG, transferrin-conjugated polyethylene glycol.
[b]Hours after convection-enhanced delivery of each BDS.
[c]The time point of 0 means the point just after rats were killed.

hemispheres and defined the normal tissue from the tumor-bearing hemisphere as ipsilateral normal brain and the normal tissue from the other hemisphere as contralateral normal brain. The normal brain of the ipsilateral side, at least a couple of millimeters away from the tumor border, was sampled with approximately 1 g for ^{10}B content measurement. The normal brain of the contralateral side, symmetrical for the ipsilateral sampling, was sampled for the measurement.

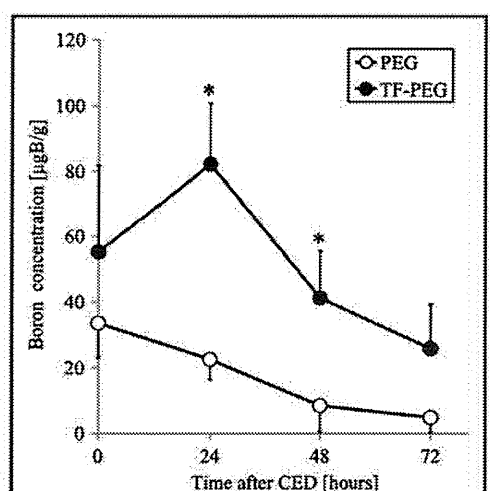

FIGURE 2. *Boron concentration of the tumor at selected times after convection-enhanced delivery (CED) administration of each boron delivery system, polyethylene glycol (PEG) liposome (sodium borocaptate [BSH], Iomeprol) or transferrin-conjugated polyethylene glycol (TF-PEG) liposome (BSH, Iomeprol). The TF-PEG group (●) and the PEG group (○). At all the time points, the tumor boron concentration in the TF-PEG group was higher than that in the PEG group. Especially at 24 and 48 hours after CED, the boron concentrations in the TF-PEG group were significantly higher than those in the PEG group (P < .05).*

Imaging Study

For the imaging study, at selected times (0, 24, 48, and 72 hours) after termination of CED, rats were analyzed by CT to evaluate the distribution of BDS and were then euthanized. In this study, we used a high-speed helical CT imaging system (Aquilion 64; Toshiba Medical Systems, Tochigi, Japan). Real-time coronal CT scans (1-mm slice thickness, 1-mm spacing) were performed. We also did a covisualization study using iodine contrast agent (Iomeprol) and fluorescence dye, co-encapsulated into the TF-PEG liposome infused by CED with the CT scan the same as for BDS.

All procedures were performed according to the Osaka Medical College Regulations on Animal Experimentation.

Statistical Analysis

Pairwise comparisons were conducted using Student's *t* test. Group differences resulting in *P* values of $<.05$ were considered statistically significant.

RESULTS

Evaluation of the Normal Rat Brain Infused BDS by CED

Fischer 344 rats receiving a 20-μg ^{10}B infusion of PEG liposome (BSH, Iomeprol) or TF-PEG liposome (BSH, Iomeprol) by CED into their right hemisphere showed no substantial evidence of adverse effects over a 14-day period. Daily observations revealed no clinical deficits during the study. The rats appeared healthy and gained or maintained body weight at the same rate as did normal rats. Histological evaluation from a representative rat euthanized on day 7 after infusion revealed some evidence of

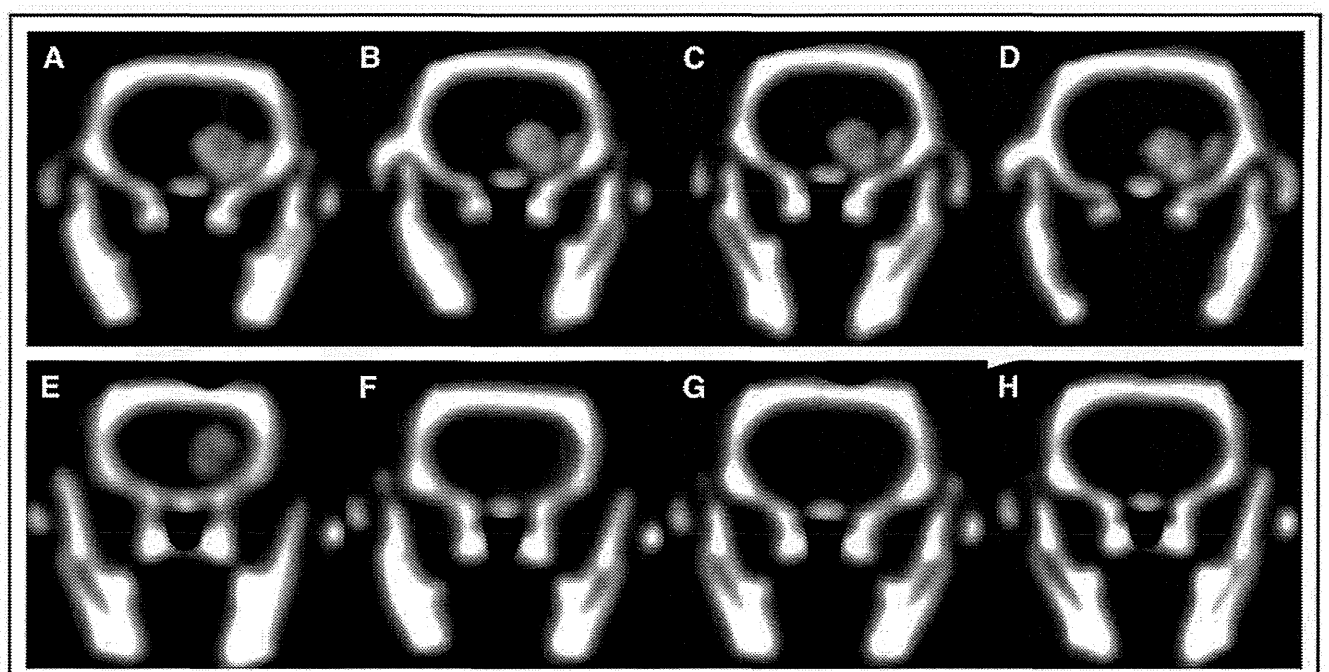

FIGURE 3. *Computed tomography (CT) imaging of iodine contrast agent distributions from each boron delivery system (BDS). These are images from CT scans at selected times (0, 24, 48, 72 hours) after the termination of convection-enhanced delivery (CED) with each BDS. The upper column (A-D) shows one of the polyethylene glycol (PEG) group, and the lower (E-H) shows one of the transferrin-conjugated polyethylene glycol (TF-PEG) group (E-H). The images are from the TF-PEG group, and the contrast enhancement was retained in the tumor until 72 hours after CED. (A-D) The images are from the PEG group. The contrast enhancement had already disappeared 24 hours after CED.*

tissue inflammation in the striatal regions proximal to the needle track on the site. This tissue reaction was observed only adjacent to the needle tract (data not shown).

In Vitro Uptake Study

The boron concentrations of F98 glioma cells 6 hours after exposure to TF-PEG liposome (BSH, Iomeprol) were significantly higher than those after exposure to PEG liposome (BSH, Iomeprol): 51.9 ± 6.8 and 16.1 ± 4.8 ng^{10}B/10^6 cells, respectively. (Figure 1) ($P < .05$).

F98 glioma line showed the minimum accumulation of BSH by TF-PEG liposomes among other glioma lines (C6, U251, U87MG, and U118MG).

In Vivo Biodistribution Study

Table 1 summarizes the biodistribution data for PEG liposome (BSH, Iomeprol) and TF-PEG liposome (BSH, Iomeprol) after CED administration to rats bearing F98 brain tumors. The boron concentrations in tumors were significantly higher in the TF-PEG group than in the PEG group at 24 and 48 hours after CED (Figure 2) ($P < .05$). Especially at 24 hours after CED, the TF-PEG group showed a higher mean tumor boron concentration (82.2 ± 18.6 μg^{10}B/g) and a higher tumor-to-normal brain ratio (274). On the other hand, at that time point, the boron concentrations of blood and contralateral normal brain were less than 1.0 μg^{10}B/g. In addition, the boron concentrations in the other organs such as liver, spleen, kidney, heart, lung, muscle, and skin were also less than 1.0 μg^{10}B/g (data not shown).

Imaging Study

Figures 3 and 4 show the results of the imaging study by CT and histological study of the brain from same rats, respectively, at 4 time points (0, 24, 48, and 72 hours). The CT images showed that the contrast enhancement of the tumor in the TF-PEG group was retained for at least until 72 hours after CED, whereas in the PEG group, the enhancement had already disappeared by 24 hours after CED. The mean Hounsfield unit values in the PEG group and the TF-PEG group were 269 ± 33.3 and 281 ± 88.4, respectively, at 0 hours, and 142 ± 40.6 and 256 ± 39.2, respectively, at 24 hours ($P < .05$) (Figure 5).

In the covisualization study using iodine contrast agent (Iomeprol) and fluorescence dye, co-encapsulated into the TF-PEG liposome administered by CED shows compatible distribution of both agents (left, fluorescencephotography; right, CT scan) (see Figure, Supplemental Digital Content 1, http://links.lww.com/NEU/A371).

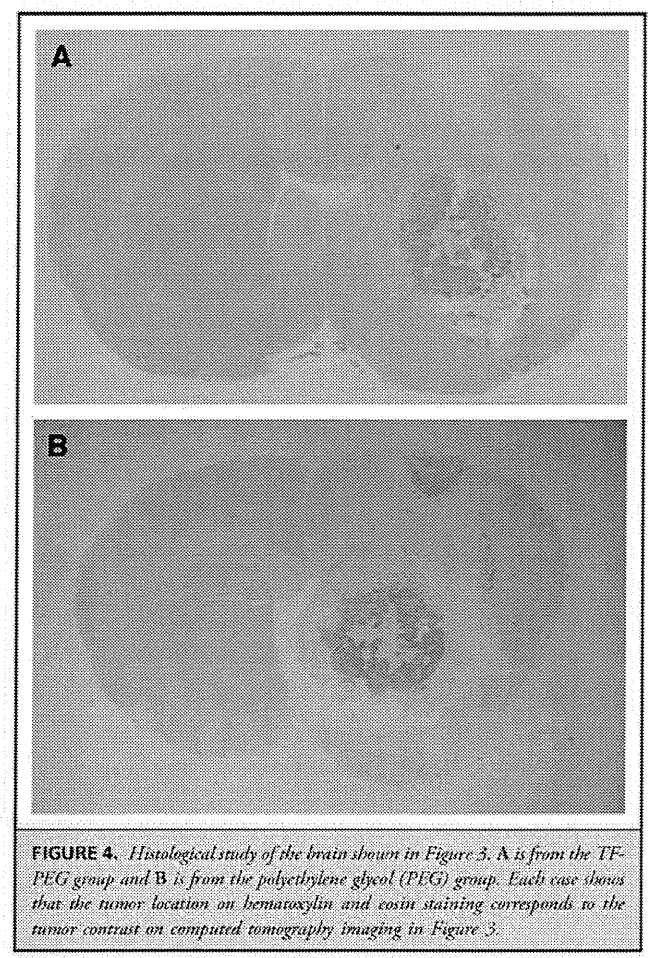

FIGURE 4. *Histological study of the brain shown in Figure 3.* A *is from the TF-PEG group and* B *is from the polyethylene glycol (PEG) group. Each case shows that the tumor location on hematoxylin and eosin staining corresponds to the tumor contrast on computed tomography imaging in Figure 3.*

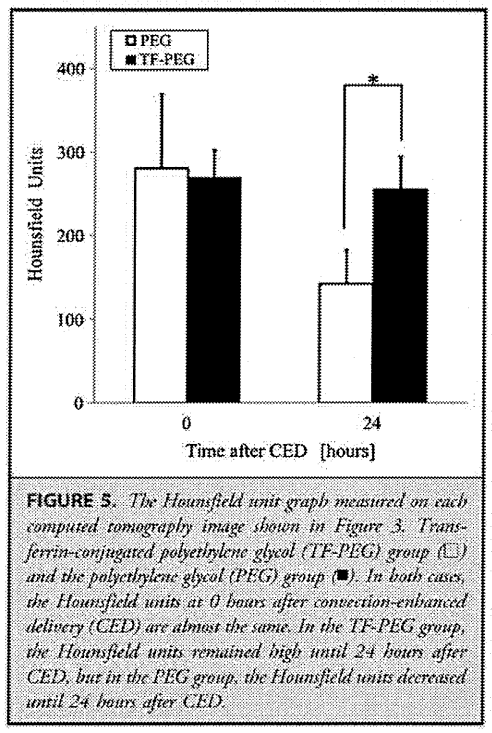

FIGURE 5. *The Hounsfield unit graph measured on each computed tomography image shown in Figure 3. Transferrin-conjugated polyethylene glycol (TF-PEG) group (□) and the polyethylene glycol (PEG) group (■). In both cases, the Hounsfield units at 0 hours after convection-enhanced delivery (CED) are almost the same. In the TF-PEG group, the Hounsfield units remained high until 24 hours after CED, but in the PEG group, the Hounsfield units decreased until 24 hours after CED.*

DISCUSSION

We previously reported that significantly higher concentrations of ^{10}B in tumor tissues in U87Δ brain tumor-bearing nude mice were achieved with systemic TF-PEG liposome (BSH) administration compared with mice administered PEG liposome (BSH) or bare BSH.[9] However, the results of that study led us to speculate on 2 problems: the limitation on ^{10}B accumulation because of the BBB, especially in the microscopic tumor cell invasion area, and the unexpected accumulation into other organs. In this study, to overcome these problems, we devised a combination of tumor targeting by transferrin and CED as a method for local drug injection directly into the brain independent of the BBB. Moreover, we devised a novel liposomal BDS that contained Iomeprol as an iodine contrast agent simultaneously with BSH to visualize the distribution of these BDSs in the brain by using CT.

The results of this in vitro boron uptake study confirmed that TF-PEG liposome can deliver BSH into F98 cells efficiently. As for the in vivo biodistribution study, we found that TF-PEG liposome can also accumulate ^{10}B at significantly high concentrations in the tumor tissue by CED, whereas low ^{10}B concentrations are maintained in normal brain, blood, and other organs. Neutron irradiation is expected to provide immeasurable tumor control efficacy by virtue of this enormously higher contrast in ^{10}B concentration to the normal brain, allowing decreased irradiation doses to the surrounding normal tissues. F98 glioma cell line showed the minimum accumulation of BSH by TF-PEG liposomes among 5 glioma cell lines tested in this study. Therefore, if we use other cell lines in vivo study, more promising results may be expected.

CED itself is a less invasive procedure, and Lonser et al[21] reported that histological inflammation was typical only within a 50-μm radius of the catheter if the agent infused was nontoxic. They also reported that CED had been proved safe in a number of species, ranging from mice to humans, and did not produce cerebral edema or measurably increased intracranial pressure. On the other hand, Saito et al[13] reported that a heterogeneous tissue arrangement of the tumor gives rise to an irregular distribution of the infused agent and to leakage into undesirable areas. They also mentioned that ideal and expected tissue distribution after CED can be significantly decreased when the catheter tip is placed near a large blood vessel, white matter tracts, or the resection cavity because of fluid escaping along the path of least resistance.

Thus, the idea of using imaging to visualize locally injected agents would logically arise. We devised a novel liposomal BDS containing Iomeprol, an iodine contrast agent, simultaneously

with BSH. Using imaging technology, such as CT, this liposomal BDS was successfully visualized and its distribution was well recognized on CT imaging even when injected into the small brain of the rat by CED.

In BNCT, unlike other therapies with cytotoxic agents such as targeted toxins[22] or anticancer drugs, the infused agent itself has no cytotoxicity until neutron irradiation is applied. So if some technical errors, such as those that Saito et al mentioned, in CED were revealed on a CT image (eg, an undesirable distribution of BDS that leaked into the cerebral ventricle or subarachnoid space), neutron irradiation could be postponed so that the safety of the therapy would be ensured. Rousseau et al[19] reported the efficacy of an iodine tracer not only as a tumor contrast agent on CT imaging but also as a dose-enhancement agent for synchrotron stereotactic radiotherapy. Their method also required precise tumor targeting, so they should have encountered the same problems as those in our study with regard to BNCT. They also adopted CED to improve iodine distribution for synchrotron stereotactic radiotherapy treatment and mentioned that its efficacy and safety in that CED can achieve high iodine concentrations in the target area and low iodine concentrations in the surrounding healthy brain tissues and blood vessels. With or without cytotoxicity of the infused agent, visualization through clinical imaging is essential for the treatment of malignant brain tumors.

In the current study, some problems arose. First, it has not been solved how the infused BDSs, liposomes, and encapsulated BSH and Iomeprol were metabolized. In Figures 2 and 4, ^{10}B concentration in tumor tissue is not proportional to Hounsfield unit value at the concerned time. This shows that there is a difference in behavior after injection between BSH and Iomeprol. If the metabolic kinetics of the BDS were disclosed, it would enable us to evaluate the ^{10}B concentration in tumor tissue by CT and Hounsfield unit value. We overcame one of the important problems of CED that caused undesirable distribution of the BDS, such as leaking into the cerebral ventricle or subarachnoid space, by co-encapsulation with drug and contrast agent for CT imaging. However, distribution of the BDS was accurately tracked by the CT imaging. Second, we could not apply neutron irradiation to evaluate the true toxicity and the therapeutic efficacy of this BDS in the current study because both reactors (KUR and JRR4) in Japan had been unavailable because of repairs and the change to uranium as fuel.

In the next step of our work, we expect to confirm that our novel strategy can obtain higher efficacy in BNCT.

Disclosure

This work was supported by Grants-in-Aid for Scientific Research for Young Scientists (B) (18791030 to S.K. and 20791022 to N.I.), by Grants-in-Aid for Scientific Research (C) (20591728 to S.K.) and (B) (19390385 to S-I.M.) from the Japanese Ministry of Education, Culture, Sports, Science and Technology, and by the Eisai Science Foundation to S.K. This work was also supported in part by the Takeda Science Foundation for Osaka Medical College. The authors have no personal financial or institutional interest in any of the drugs, materials, or devices described in this article.

REFERENCES

1. Miyatake S, Kawabata S, Nonoguchi N, et al. Pseudoprogression in boron neutron capture therapy for malignant gliomas and meningiomas. *Neuro Oncol.* 2009;11(4):430-436.
2. Miyatake S, Kawabata S, Yokoyama K, et al. Survival benefit of Boron neutron capture therapy for recurrent malignant gliomas. *J Neurooncol.* 2009;91(2):199-206.
3. Miyatake S, Kawabata S, Kajimoto Y, et al. Modified boron neutron capture therapy for malignant gliomas performed using epithermal neutron and two boron compounds with different accumulation mechanisms: an efficacy study based on findings on neuroimages. *J Neurosurg.* 2005;103(6):1000-1009.
4. Kawabata S, Miyatake S, Kajimoto Y, et al. The early successful treatment of glioblastoma patients with modified boron neutron capture therapy. Report of two cases. *J Neurooncol.* 2003;65(2):159-165.
5. Kawabata S, Miyatake S, Kuroiwa T, et al. Boron neutron capture therapy for newly diagnosed glioblastoma. *J Radiat Res (Tokyo).* 2009;50(1):51-60.
6. Barth RF, Coderre JA, Vicente MG, Blue TE. Boron neutron capture therapy of cancer: current status and future prospects. *Clin Cancer Res.* 2005;11(11):3987-4002.
7. Wei Q, Kullberg EB, Gedda L. Trastuzumab-conjugated boron-containing liposomes for tumor-cell targeting; development and cellular studies. *Int J Oncol.* 2003;23(4):1159-1165.
8. Yang W, Barth RF, Adams DM, et al. Convection-enhanced delivery of boronated epidermal growth factor for molecular targeting of EGF receptor-positive gliomas. *Cancer Res.* 2002;62(22):6552-6558.
9. Doi A, Kawabata S, Iida K, et al. Tumor-specific targeting of sodium borocaptate (BSH) to malignant glioma by transferrin-PEG liposomes: a modality for boron neutron capture therapy. *J Neurooncol.* 2008;87(3):287-294.
10. Bobo RH, Laske DW, Akbasak A, Morrison PF, Dedrick RL, Oldfield EH. Convection-enhanced delivery of macromolecules in the brain. *Proc Natl Acad Sci U S A.* 1994;91(6):2076-2080.
11. Wu G, Barth RF, Yang W, Kawabata S, Zhang L, Green-Church K. Targeted delivery of methotrexate to epidermal growth factor receptor-positive brain tumors by means of cetuximab (IMC-C225) dendrimer bioconjugates. *Mol Cancer Ther.* 2006;5(1):52-59.
12. Mukundan S Jr, Ghaghada KB, Badea CT, et al. A liposomal nanoscale contrast agent for preclinical CT in mice. *AJR Am J Roentgenol.* 2006;186(2):300-307.
13. Saito R, Bringas JR, McKnight TR, et al. Distribution of liposomes into brain and rat brain tumor models by convection-enhanced delivery monitored with magnetic resonance imaging. *Cancer Res.* 2004;64(7):2572-2579.
14. Dickinson PJ, LeCouteur RA, Higgins RJ, et al. Canine model of convection-enhanced delivery of liposomes containing CPT-11 monitored with real-time magnetic resonance imaging: laboratory investigation. *J Neurosurg.* 2008;108(5):989-998.
15. Aoki I, Bakalova R. MR molecular imaging using drug delivery system. *Drug Delivery System.* 2008;23(1):61-68.
16. Weaver M, Laske DW. Transferrin receptor ligand-targeted toxin conjugate (Tf-CRM107) for therapy of malignant gliomas. *J Neurooncol.* 2003;65(1):3-13.
17. Murad GJ, Walbridge S, Morrison PF, et al. Real-time, image-guided, convection-enhanced delivery of interleukin 13 bound to pseudomonas exotoxin. *Clin Cancer Res.* 2006;12(10):3145-3151.
18. Vogelbaum MA. Convection enhanced delivery for the treatment of malignant gliomas: symposium review. *J Neurooncol.* 2005;73(1):57-69.
19. Rousseau J, Boudou C, Esteve F, Elleaume H. Convection-enhanced delivery of an iodine tracer into rat brain for synchrotron stereotactic radiotherapy. *Int J Radiat Oncol Biol Phys.* 2007;68(3):943-951.
20. Maruyama K, Ishida O, Kasaoka S, et al. Intracellular targeting of sodium mercaptoundecahydrododecaborate (BSH) to solid tumors by transferrin-PEG liposomes, for boron neutron-capture therapy (BNCT). *J Control Release.* 2004;98(2):195-207.
21. Lonser RR, Walbridge S, Garmestani K, et al. Successful and safe perfusion of the primate brainstem: in vivo magnetic resonance imaging of macromolecular distribution during infusion. *J Neurosurg.* 2002;97(4):905-913.
22. Rainov NG, Soling A. Clinical studies with targeted toxins in malignant glioma. *Rev Recent Clin Trials.* 2006;1(2):119-131.

***Supplemental digital content** is available for this article. Direct URL citations appear in the printed text and are provided in the HTML and PDF versions of this article on the journal's Web site (www.neurosurgery-online.com).*

Acknowledgments

We thank Dr Rolf F. Barth, Department of Pathology, The Ohio State University, for preparing the F98 cell line and Hiromi Kuroda for technical assistance.

COMMENTS

The authors report a novel means to introduce potential sensitizing agents into an experimental brain tumor in an animal model using convection-enhanced delivery. The goal is to introduce these potential agents into the brain surrounding a tumor mass and eventually administer neutron radiation with the hope of providing greater cell kill, especially in the infiltrated zone. In essence, this is a study showing that specially tailored pharmaceuticals can be created to increase delivery of a selected agent in the target zone and that addition of other agents may make recognition of the target by imaging possible as well. It would be even better to demonstrate in a part 2 study that this targeting of sensitizing compounds actually resulted in a therapeutic response using boron neutron capture therapy (BCNT). This technology has been advocated in a relatively few centers for more than 40 years; perhaps because of the large overhead cost and lack of major therapeutic safety window, it has never reached mainstream use. Further efforts may allow safer BNCT, especially because the authors show that tissue concentrations are significantly reduced in other tissues, an important feature that may improve the safety of BNCT during the actual radiation administration. The risk-benefit ratio in BNCT has been difficult to ascertain. In the past, neutron radiation was effective at killing the target tumor but usually resulted in unacceptable radiation toxicity in the brain. Perhaps further efforts in this field will yet allow a beneficial therapeutic window to emerge.

L. D. Lunsford
Pittsburgh, Pennsylvania

The authors describe their early preclinical findings (in vitro and in vivo) in a potentially interesting application and modification of BCNT. Their strategy directly targets glioma cells (and the surrounding region) with transferrin bound to a polyethylene glycol liposome that encapsulates sodium borocaptate and an iodine contrast agent (used for tracking the liposome distribution during computed tomography imaging). To provide high concentrations of this compound to regions in and around glioma, it was delivered to tumor and surrounding region via convection-enhanced delivery.

The data from this study indicate that the polyethylene glycol liposome encapsulated sodium borocaptate can be safely and successfully delivered by convection-enhanced delivery in rodent brain tumor models while tracking its distribution using computed tomography imaging. Although these early findings are encouraging from a distribution perspective, the next potential step in determining whether this modification of BCNT for glioma may hold promise will be in determining therapeutic dosing (irradiation) and assessing efficacy in vivo. I look forward to the authors' subsequent work in this area.

Russell R. Lonser
Bethesda, Maryland

J Neurooncol (2011) 102:471–475
DOI 10.1007/s11060-010-0333-3

CASE REPORT

Repeated treatments with bevacizumab for recurrent radiation necrosis in patients with malignant brain tumors: a report of 2 cases

Motomasa Furuse · Shinji Kawabata · Toshihiko Kuroiwa · Shin-Ichi Miyatake

Received: 26 April 2010 / Accepted: 23 July 2010 / Published online: 7 August 2010

Abstract Bevacizumab is expected to constitute a new treatment modality for radiation necrosis. In the present cases, we observed a recurrence of radiation necrosis after temporary improvement by bevacizumab treatment. Re-treatment with bevacizumab controlled the necrosis again. A 39-year-old male and a 57-year-old female were diagnosed with glioblastoma and lung cancer metastasis, respectively. The former patient underwent partial resection of the glioblastoma, followed by boron neutron capture therapy (BNCT) and 30 Gy of fractionated X-ray radiotherapy. Eleven months after BNCT, he suffered from left hemiparesis and convulsions with enlargement of a perifocal edema. The latter patient underwent stereotactic radiosurgery twice for the same tumor. Three months after the second radiosurgery, she had an uncontrollable convulsion and right hemiplegia with a massive perifocal edema. Both lesions were suggested to be radiation necroses by positron emission tomography using amino acids as a tracer. Neither patient responded to corticosteroids, anticoagulants, or vitamin E. They underwent treatment with 5 mg/kg bevacizumab biweekly, for a total of 6 cycles. The size of the perifocal edema was clearly reduced in response to the treatments. The neurological status of the patients improved concomitant with therapy. However, the clinical status of both patients was aggravated several months after the bevacizumab was stopped, and the perifocal edemas enlarged again. The patients underwent a second treatment with bevacizumab, and the perifocal edemas again decreased. Although radiation necrosis may recur several months after bevacizumab treatment, repeated bevacizumab treatments also appear to be effective.

Keywords Bevacizumab · Boron neutron capture therapy · Brain edema · Glioblastoma, metastatic brain tumor · Radiation necrosis

Bevacizumab is a humanized murine monoclonal antibody against the vascular endothelial growth factor (VEGF) ligand that has been approved by the FDA in the U.S. to treat colorectal cancer, non-small cell lung cancer, renal cancer, breast cancer, and glioblastoma multiforme [1–5]. In addition, preliminary studies reported that bevacizumab was effective for treating radiation necrosis in the central nervous system [6, 7]. These studies led to a randomized controlled trial that demonstrated class I evidence of the efficacy of bevacizumab treatment for progressive radiation necrosis [8]. In the present work, we report our use of bevacizumab to treat two patients who showed signs of radiation necrosis after radiotherapy for a metastatic brain tumor and a glioblastoma, respectively. In both cases, rapid improvement was achieved both clinically and neuroradiologically after the initial treatment, but the patients worsened several months after the bevacizumab treatment was stopped, and thus a second round of bevacizumab therapy was used. We report the results of these two cases.

Case 1

A 39-year-old male had a right parietal cystic glioblastoma. Fluoride-labeled boronophenylalanine (BPA)-positron emission tomography (PET) was applied for the residual lesion, and the lesion/normal tissue (L/N) ratio was 3.0

M. Furuse · S. Kawabata · T. Kuroiwa · S.-I. Miyatake (✉)
Department of Neurosurgery, Osaka Medical College, 2-7, Daigakumachi, Takatsuki, Osaka 569-8686, Japan
e-mail: neu070@poh.osaka-med.ac.jp

(Fig. 1a). This L/N ratio was representative of glioblastoma [9]. An L/N ratio of greater than 2.5 is strongly suggestive of tumor progression in newly-diagnosed or recurrent glioblastomas, while an L/N ratio of less than 2.0 suggests a high possibility of radiation necrosis or pseudoprogression [9, 10]. Tumor-selective particle radiation, boron neutron capture therapy (BNCT) were applied with a minimum tumor dose of 42.3 Gy-Eq and a maximum brain dose of 11.9 Gy-Eq [10, 11]. Here, Gy-Eq (gray-equivalent) corresponds to an X-ray dose that can yield effects equivalent to total BNCT radiation [10]. This treatment was followed by 30 Gy fractionated X-ray treatment, according to our recent protocol [12], and temozolomide as adjuvant chemotherapy. The residual tumor was decreased in size in follow-up magnetic resonance (MR) images.

Eleven months after BNCT, left hemiparesis and convulsions recurred and the MR images showed re-enlargement of the gadolinium-enhanced lesion with perifocal edema (Fig. 2a, b). BPA-PET was re-applied to determine whether the lesion represented a radiation necrosis or local tumor progression. The L/N ratio in this PET was 1.9, which suggested that the lesion was indeed radiation necrosis (Fig. 1b) [9]. Corticosteroids, anticoagulants, and vitamin E were all tried and were not effective.

The patient underwent treatment with bevacizumab of 5 mg/kg biweekly for 6 cycles in total. MR images revealed that the perilesional edema and gadolinium-enhanced lesion were reduced in size, as shown in Fig. 2c,d. The convulsions were controlled with anticonvulsants, and the hemiparesis improved without use of glucocorticoids.

The patient was restarted on treatment with anticoagulants and vitamin E. Six months later, however, his neurological status was aggravated and MR images demonstrated abnormal enhancement and progression of the perifocal edema (Fig. 3a, b). BPA-PET yielded an L/N ratio of 2.1, suggesting the recurrence of radiation necrosis (Fig. 1c). The L/N ratios in Fig. 2b and c were almost the same (1.9 and 2.1), and compatible with radiation necrosis. He was again treated with 5 mg/kg of bevacizumab every other week. After 3 cycles of bevacizumab, MR images again demonstrated a decrease in the perifocal edema and post-gadolinium enhancement (Fig. 3c, d), and the treatment was stopped. At the time of this writing, the patient has been doing well for more than 4 months without worsening of clinical symptoms.

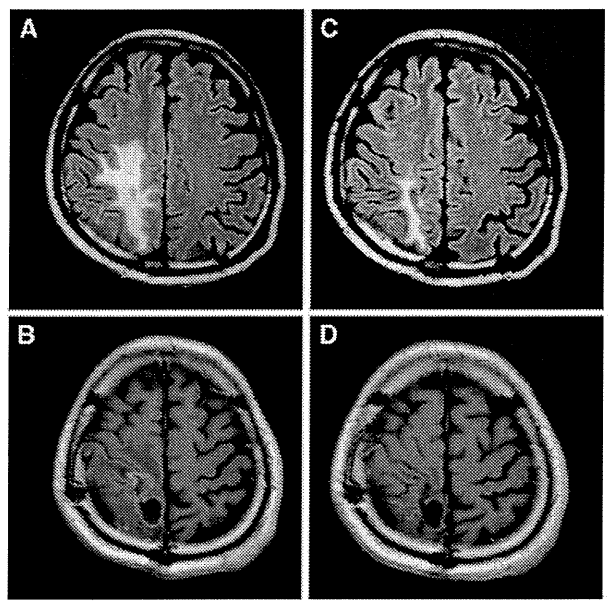

Fig. 2 FLAIR MR images before treatment of bevacizumab (**a**), and after 6 cycles of bevacizumab 5 mg/kg (**c**). Postcontrast T1-weighted MR images before treatment with bevacizumab (**b**), and after 6 cycles of bevacizumab 5 mg/kg (**d**). *Upper row* an extended hyperintense area obviously reduced after bevacizumab treatment. *Lower row* a postcontrast enhanced lesion indistinct after bevacizumab treatment

Case 2

A 57-year-old female experienced a seizure and was diagnosed with a brain metastasis in the left motor strip, which was derived from lung cancer. She underwent repetitive stereotactic radiosurgery (SRS) with a total marginal dose of 49 Gy over a 6-month interval. Three months after the second SRS, her seizures became uncontrollable and right hemiplegia occurred. MR images revealed a progression of perifocal edema and an enhanced lesion (Fig. 4a, b).

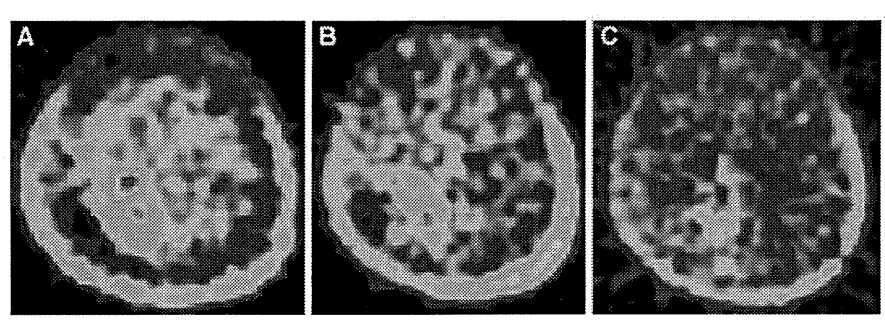

Fig. 1 Serial BPA-PET study in Case 1. **a**: BPA-PET just prior to BNCT (L/N ratio: 3.0). **b**: BPA-PET taken at the first aggravation of clinical symptoms and neuroimages (L/N ratio: 1.9). **c**: BPA-PET taken at the 2nd aggravation (L/N ratio: 2.1)

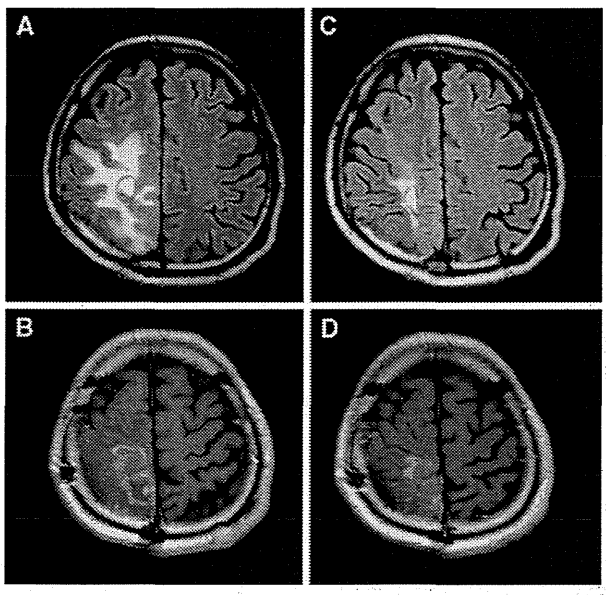

Fig. 3 FLAIR MR images before the second treatment with bevacizumab (**a**) and after 3 cycles of bevacizumab 5 mg/kg (**c**). Postcontrast T1-weighted MR images before the second treatment with bevacizumab (**b**) and after 3 cycles of bevacizumab 5 mg/kg (**d**). *Upper row* an enlarged hyperintense area apparently decreased after the second bevacizumab treatment. *Lower row* postcontrast enhancement became vague after the second bevacizumab treatment

BPA-PET showed a low uptake of BPA, and an L/N ratio of 1.8. Together with the MR findings, these results suggested that the lesion was a radiation necrosis. Her clinical symptoms did not respond to increasing doses of steroids or other medical treatments.

She was treated with 5 mg/kg of bevacizumab every other week. MR images obtained 1 week after one dose showed a dramatic reduction in the hyperintense area on fluid-attenuated inversion recovery (FLAIR) images and attenuation of the abnormal enhanced area on gadolinium-enhanced T1-weighted images (Fig. 4c, d). Subsequent MR images were obtained 1 week after 6 cycles and demonstrated a further decrease in the FLAIR-hyperintense lesion (Fig. 4e). The patient's hemiparesis consistently improved, and she was able to walk by herself. Her performance status improved from grade 2 to grade 3.

At this time, her treatment was reduced to simply anticoagulants and vitamin E. Three months later, her hemiparesis was aggravated and computed tomographic imaging revealed an enlarged low-density area (Fig. 5a). She underwent a second bevacizumab treatment. After 2 cycles of bevacizumab, the MR images showed a decrease in perifocal edema (Fig. 5b), but new multiple metastatic lesions. The bevacizumab treatment was therefore discontinued.

Discussion

Recently, new radiation therapies, such as BNCT, SRS, proton beam radiation, and intensity-modulated radiation therapy, have been performed for patients with malignant gliomas. These high-dose radiation therapeutics have been improving patient survival [11–14], but radiation necrosis in the brain has become a more serious problem. Current treatments for radiation necrosis of the brain include the

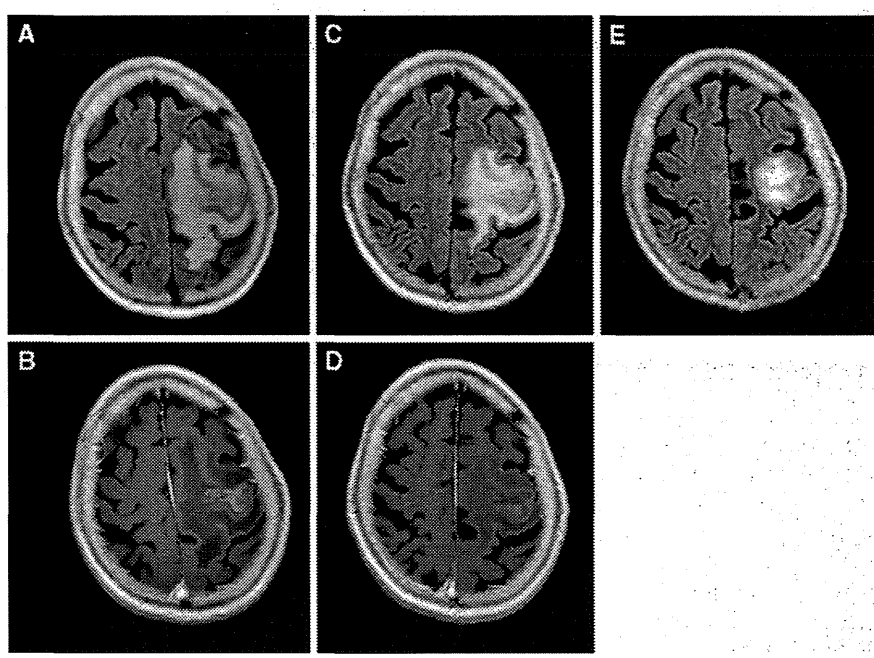

Fig. 4 FLAIR MR images before treatment with bevacizumab (**a**), 1 week after one dose of bevacizumab 5 mg/kg (**c**), and after 6 cycles (**e**). Postcontrast T1-weighted MR images before treatment with bevacizumab (**b**) and 1 week after one dose of bevacizumab 5 mg/kg (**d**). *Upper row* a hyperintense area progressively and dramatically reduced after administration of bevacizumab. *Lower row* a postcontrast enhancement obscured after bevacizumab treatment

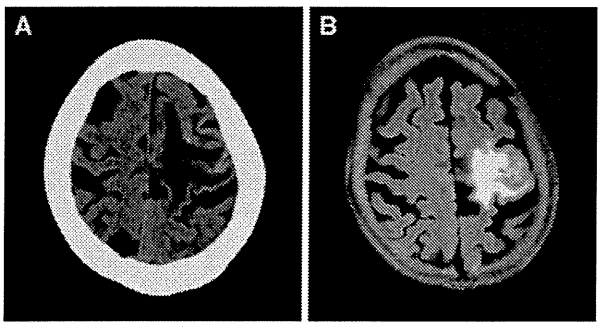

Fig. 5 A computed tomographic image 3 months after the first bevacizumab treatment (**a**) and a FLAIR MR image after 2 cycles of the second bevacizumab treatment (**b**). A perilesional edema decreased after the second bevacizumab treatment

use of corticosteroids, anticoagulants, and vitamin E, as well as hyperbaric oxygenation and surgical resection [15–19]. Corticosteroids are often effective in the early phase of radiation injury, but are ineffectual in late radiation injury. Radiation injury includes damage of the vascular endothelial cells, leading to an increase in vascular permeability [20, 21]. Bevacizumab is theoretically effective against radiation injury because VEGF is known as a vascular permeability factor [22]. Gonzalez et al. [6] first reported the effects of bevacizumab on radiation necrosis of brain tumors. They reviewed the cases of 8 patients with recurrent malignant gliomas and radiation necrosis who were treated with bevacizumab, and in some cases with temozolomide or other anticancer agents as well, Radiation necrosis was diagnosed by biopsy in 2 of these patients and by MR images in 6. All 8 patients showed improvement on MR images within 8 weeks of the bevacizumab treatment. Another report by Torcuator et al. [7] also demonstrated the effectiveness of bevacizumab on cerebral radiation necrosis. They confirmed radiation necrosis by biopsy in all 6 patients. Neither of these earlier reports mentioned whether or not radiation necrosis recurred.

In the present case reports, radiation necrosis recurred several months after bevacizumab treatment in both patients. Our patients showed the same initial response to bevacizumab as in the two previous reports. However, in our cases, the bevacizumab treatment did not permanently eradicate the radiation necrosis, and the necrosis recurred. We found bevacizumab effective in treating recurrent radiation necrosis. In the study reported by Levin et al. [8], three patients benefited by retreatment with bevacizumab. In our report, we also found that radiation necrosis can be controlled with bevacizumab treatment as initial treatment as well as in the event of post-bevacizumab recurrence of radiation necrosis.

Our diagnosis of radiation necrosis was based on BPA-PET and serial MR images. Although the findings of BPA-PET were correlated to histopathological results in our previous study [9], BPA-PET is not a proven radiographic modality. Therefore, our patients were presumed to have radiation necrosis, because the histopathological findings of biopsy or surgical resection are considered definitive for a diagnosis of radiation necrosis. Surgical resection is an important modality if brain edema does not respond to medical treatment and the lesions are resectable. In one of the present cases, because the lesion itself involved the motor strip, a lesionectomy was out of the question. Based on the present findings, bevacizumab can be considered a new treatment modality for both new and recurrent radiation necrosis of the brain, especially for unresectable lesions, as shown here. Its use would influence not only the treatment strategy for radiation necrosis, but also radiotherapeutic dose planning for unresectable tumors.

Conclusion

We used bevacizumab in the treatment of two patients with radiation necrosis of brain tumors. Several months later, however, radiation necrosis recurred in both patients. Repeated therapy with bevacizumab was similarly effective against the recurrent radiation necrosis. Moreover, bevacizumab appears to be an effective treatment for radiation necrosis, especially for lesions located in an eloquent area because radiation necrosis in this area is surgically inaccessible.

Acknowledgments This work was partly supported by a Grant-in-Aid for Scientific Research (B) (19390385 to S.I.M.) from the Japanese Ministry of Education, Science and Culture and in part by the Takeda Science Foundation for Osaka Medical College.

References

1. Hurwitz H, Fehrenbacher L, Novotny W, Cartwright T, Hainsworth J, Heim W, Berlin J, Baron A, Griffing S, Holmgren E, Ferrara N, Fyfe G, Rogers B, Ross R, Kabbinavar F (2004) Bevacizumab plus irinotecan, fluorouracil, and leucovorin for metastatic colorectal cancer. N Engl J Med 350:2335–2342
2. Sander A, Gray R, Perry MC, Brahmer J, Schiller JH, Dowlati A, Lilenbaum R, Johnson DH (2006) Paclitaxel-carboplatin alone or with bevacizumab for non-small-cell lung cancer. N Engl J Med 355:2542–2550
3. Escudier B, Pluzanska A, Koralewski P, Ravaud A, Bracarda S, Szczlik C, Chevreau C, Filipek M, Melichar B, Bajetta E, Gorbunova V, Bay JO, Bodrogi I, Jagiello-Gruszfeld A, Moore N, AVOREN Trial Investigators (2007) Bevacizumab plus interferon alfa-2a for treatment of metastatic renal cell carcinoma: a randomized, double-blind phase III trial. Lancet 370:2103–2111
4. Miller KD, Chap LI, Holmes FA, Cobleigh MA, Marcom PK, Fehrenbacher L, Dickler M, Overmoyer BA, Reimann JD, Sing AP, Langmuir V, Rugo HS (2005) Randomized phase III trial of capecitabine compared with bevacizumab plus capecitabine in

patients with previously treated metastatic breast cancer. J Clin Oncol 23:792–799
5. Vredenburgh JJ, Desjardins A, Herndon JE IId, Marcello J, Reardon DA, Quinn JA, Rich JN, Sathornsumetee S, Gururangan S, Sampson J, Wagner M, Bailey L, Bigner DD, Friedman AH, Friedman HS (2007) Bevacizumab plus irinotecan in recurrent glioblastoma multiforme. J Clin Oncol 25:4722–4729
6. Gonzalez J, Kumar AJ, Conrad CA, Levin VA (2007) Effect of bevacizumab on radiation necrosis of the brain. Int J Radiat Oncol Biol Phys 67:323–326
7. Torcuator R, Zuniga R, Mohan YS, Rock J, Doyle T, Anderson J, Gutierrez J, Ryu S, Jain R, Rosenblum M, Mikkelsen T (2009) Initial experience with bevacizumab treatment for biopsy confirmed cerebral radiation necrosis. J Neurooncol 94:63–68
8. Levin VA, Bidaut L, Hou P, Kumar AJ, Wefel JS, Bekele N, Prabhu S, Loghin M, Gilbert MR, Jackson EF (2010) Randomized double-blind placebo-controlled trial of bevacizumab therapy for radiation necrosis of the central nervous system. Int J Radiat Oncol Biol Phys. doi:10.1016/j.ijrobp.2009.12.061
9. Miyashita M, Miyatake S, Imahori Y, Yokoyama K, Kawabata S, Kajimoto Y, Shibata MA, Otsuki Y, Kirihata M, Ono K, Kuroiwa T (2008) Evaluation of fluoride-labeled boronophenylalanine-PET imaging for the study of radiation effects in patients with glioblastomas. J Neurooncol 89:239–246
10. Miyatake S, Kawabata S, Nonoguchi N, Yokoyama K, Kuroiwa T, Matsui H, Ono K (2009) Pseudoprogression in boron neutron capture therapy for malignant gliomas and meningiomas. Neurooncology 11:430–436
11. Miyatake S, Kawabata S, Kajimoto Y, Aoki A, Yokoyama K, Yamada M, Kuroiwa T, Tsuji M, Imahori Y, Kirihata M, Sakurai Y, Masunaga S, Nagata K, Maruhashi A, Ono K (2005) Modified boron neutron capture therapy for malignant gliomas performed using epithermal neutron and two boron compounds with different accumulation mechanisms: an efficacy study based on findings on neuroimages. J Neurosurg 103:1000–1009
12. Kawabata S, Miyatake SI, Kuroiwa T, Yokoyama K, Doi A, Iida K, Miyata S, Nonoguchi N, Michiue H, Takahashi M, Inomata T, Imahori Y, Kirihata M, Sakurai Y, Maruhashi A, Kumada H, Ono K (2009) Boron neutron capture therapy for newly diagnosed glioblastoma. J Radiat Res (Tokyo) 50:51–60
13. Fitzek MM, Thornton AF, Rabinov JD, Lev MH, Pardo FS, Munzenrider JE, Okunieff P, Bussiere M, Braun I, Hochberg FH, Hedley-Whyte ET, Liebsch NJ, Harsh GR IV (1999) Accelerated fractionated proton/photon irradiation to 90 cobalt gray equivalent for glioblastoma multiforme: results of a phase II prospective trial. J Neurosurg 91:251–260
14. Iuchi T, Hatano K, Narita Y, Kodama T, Yamaki T, Osato K (2006) Hypofractionated high-dose irradiation for the treatment of malignant astrocytomas using simultaneous integrated boost technique by IMRT. Int J Radiat Oncol Biol Phys 64:1317–1324
15. Delanian S, Balla-Mekias S, Lefaix JL (1999) Striking regression of chronic radiotherapy damage in a clinical trial of combined pentoxifylline and tocopherol. J Clin Oncol 17:3283–3290
16. Glantz MJ, Burger PC, Friedman AH, Radtke RA, Massey EW, Schold SC Jr (1994) Treatment of radiation-induced nervous system injury with heparin and warfarin. Neurology 44:2020–2027
17. Rizzoli HV, Pagnanelli DM (1984) Treatment of delayed radiation necrosis of the brain. A clinical observation. J Neurosurg 60:589–594
18. Shaw PJ, Bates D (1984) Conservative treatment of delayed cerebral radiation necrosis. J Neurol Neurosurg Psychiatry 47:1338–1341
19. Tandon N, Vollmer DG, New PZ, Hevezi JM, Herman T, Kagan-Hallet K, West GA (2001) Fulminant radiation-induced necrosis after stereotactic radiation therapy to the posterior fossa. Case report and review of the literature. J Neurosurg 95:507–512
20. Coderre JA, Morris GM, Micca PL, Hopewell JW, Verhagen I, Kleiboer BJ, van der Kogel AJ (2006) Late effects of radiation on the central nervous system: role of vascular endothelial damage and glial stem cell survival. Radiat Res 166:495–503
21. Kimura T, Sako K, Tohyama Y, Aizawa S, Yoshida H, Aburano T, Tanaka K, Tanaka T (2003) Diagnosis and treatment of progressive space-occupying radiation necrosis following stereotactic radiosurgery for brain metastasis: value of proton magnetic resonance spectroscopy. Acta Neurochir (Wien) 145:557–564
22. Midgley R, Kerr D (2005) Bevacizumab—current status and future directions. Ann Oncol 16:999–1004

Applied Radiation and Isotopes 69 (2011) 1721–1724

Contents lists available at ScienceDirect

Applied Radiation and Isotopes

journal homepage: www.elsevier.com/locate/apradiso

Boron neutron capture therapy for clear cell sarcoma (CCS): Biodistribution study of *p*-borono-L-phenylalanine in CCS-bearing animal models

T. Andoh [a], T. Fujimoto [b], T. Sudo [c], I. Fujita [b], M. Imabori [b], H. Moritake [d], T. Sugimoto [e], Y. Sakuma [f], T. Takeuchi [g], S. Kawabata [h], M. Kirihata [i], T. Akisue [j], K. Yayama [k], M. Kurosaka [j], S. Miyatake [h], Y. Fukumori [a], H. Ichikawa [a,*]

[a] *Laboratory of Pharmaceutical Technology, Faculty of Pharmaceutical Sciences and Cooperative Research Center of Life Sciences, Kobe Gakuin University, Kobe 650-8586, Japan*
[b] *Department of Orthopaedic Surgery, Hyogo Cancer Center, Akashi 673-0021, Japan*
[c] *Section of Translational Research, Hyogo Cancer Center, Akashi 673-0021, Japan*
[d] *Department of Pediatrics, Miyazaki University, Kiyotake 889-1692, Japan*
[e] *Department of Pediatrics, Saiseikai Shigaken Hospital, Ritto 520-3046, Japan*
[f] *Department of Pathology, Hyogo Cancer Center, Akashi 673-0021, Japan*
[g] *Department of Pathology, Kochi University, Nangoku 783-8505, Japan*
[h] *Department of Neurosurgery, Osaka Medical College, Osaka 569-8686, Japan*
[i] *Graduate School of Life and Environmental Sciences, Osaka Prefecture University, Sakai 599-8531, Japan*
[j] *Department of Orthopaedic Surgery, Kobe University Graduate School of Medicine, Kobe 650-0017, Japan*
[k] *Laboratory of Cardiovascular Pharmacology, Faculty of Pharmaceutical Sciences and Cooperative Research Center of Life Sciences, Kobe Gakuin University, Kobe 650-8586, Japan*

ARTICLE INFO

Available online 1 March 2011

Keywords:
Biodistribution
p-Borono-L-phenylalanine
Clear cell sarcoma
MP-CCS-SY
Boron neutron capture therapy
Anti-BPA monoclonal antibody

ABSTRACT

Clear cell sarcoma (CCS) is a rare melanocytic malignant tumor with a poor prognosis. Our previous study demonstrated that *in vitro* cultured CCS cells have the ability to highly uptake L-BPA and thus boron neutron capture therapy could be a new option for CCS treatment. This paper proved that a remarkably high accumulation of ^{10}B (45–74 ppm) in tumor was obtained even in a CCS-bearing animal with a well-controlled biodistribution followed by intravenous administration of L-BPA-fructose complex (500 mg BPA/kg).

1. Introduction

Clear cell sarcoma (CCS), a rare melanocytic malignant tumor with a predilection for young adults, is of poor prognosis. Since its treatment other than surgical resection is lacking, a new clinical approach for its management is required (Weiss and Goldblum, 2001).

Melanoma cells preferentially take up *p*-borono-L-phenylalanine (L-BPA) because its chemical structure is similar to tyrosine required for melanogenesis. Therefore, L-BPA has been used in boron neutron capture therapy (BNCT) for malignant melanoma (Mishima et al., 1989). CCS is also capable of producing melanin. Similarity in melannogensis between melanoma and CCS promises high BPA uptake by CCS. Indeed, we have proved that remarkable uptake of BPA with an extremely high level, i.e., 80 μg ^{10}B/g cells, took place when CCS was exposed to BPA-containing cell culture medium *in vitro* (Fujimoto et al., in press). Thus, BNCT using L-BPA is expected to be a new clinical option for the treatment of CCS, provided that such a high accumulation of boron in CCS can be realized even in vivo under a well-controlled biodistribution of L-BPA.

In the present study, we are aiming at investigating *in vivo* biodistribution of L-BPA in a CCS-bearing animal model. For this purpose, CCS cell line of human origin (MP-CCS-SY) was employed and a CCS-bearing animal model was established by subcutaneous transplantation of MP-CCS-SY to nude mice. Biodistribution of L-BPA followed by its intravenous administration into the CCS-bearing nude mice thus obtained was evaluated. Additionally, the tumor resected from the BPA-given mice was assessed with immunohistological examination using anti-BPA monoclonal antibody to visualize microscopic distribution of BPA in the tumor tissue.

2. Materials and methods

2.1. Chemicals

L-BPA (^{10}B enriched) was kindly supplied by Stella Pharma Corporation (Osaka, Japan). Fructose, perchloric acid ($HClO_4$, 60%),

* Corresponding author. Tel.: +81 78 974 1551; fax: +81 78 974 4814.
E-mail address: ichikawa@pharm.kobegakuin.ac.jp (H. Ichikawa).

0969-8043/$ - see front matter © 2011 Elsevier Ltd. All rights reserved.
doi:10.1016/j.apradiso.2011.02.005

hydrogen peroxide (H_2O_2, 30%) and boron standard solution (1000 μg/mL) were purchased from Nacalai Tesque, Inc. (Kyoto, Japan). L-BPA was used as a fructose complex (BPA-Fr, 4000 μg ^{10}B/mL) (Yoshino et al., 1989). Anti-BPA monoclonal antibody (anti-BPA MAb) was obtained as a self-made product (Kirihata and Asano 2008). LSAB2 kit/HRP (DAB) was purchased from DAKO Japan, Inc. (Kyoto, Japan).

2.2. Cell

The MP-CCS-SY established from the bone metastatic tissue of a 17-years-old girl was employed as a human CCS cell line (Moritake et al., 2002). The melanogenesis of MP-CCS-SY has been reported previously: the melanosome was identified by electron-microscopic appearance and indirect immunofluorescence for melanoma-associated antigens (Moritake et al., 2002). The MP-CCS-SY cells were cultured in RPMI-1640 medium containing penicillin (100 U/mL), streptomycin (100 μg/mL) and 10% heat-inactivated fetal bovine serum, and incubated in a humidified atmosphere of 5% CO_2 in air at 37 °C.

2.3. Animal and tumor

All animal experiments were performed according to the regulations of the Animal Care and Use Committee of Kobe Gakuin University (Kobe, Japan). Four-weeks-old female BALB/cAJcl-nu/nu nude mice (body weight of approx. 15 g) were purchased from CLEA Japan, Inc. In order to establish CCS-bearing animal models, 0.1 mL of the culture medium containing 1×10^7 MP-CCS-SY cells was subcutaneously (s.c.) implanted into the dorsal or femoral region of the nude mice. These two models were used in biodistibution studies of L-BPA.

2.4. Biodistribution of BPA-Fr

When the MP-CCS-SY tumor in each mouse (body weight of approximately 20 g) grew to about 10 mm in diameter (approximately four weeks after MP-CCS-SY cells implantation), BPA-Fr (500 mg BPA/kg) was intravenously (i.v.) administered via

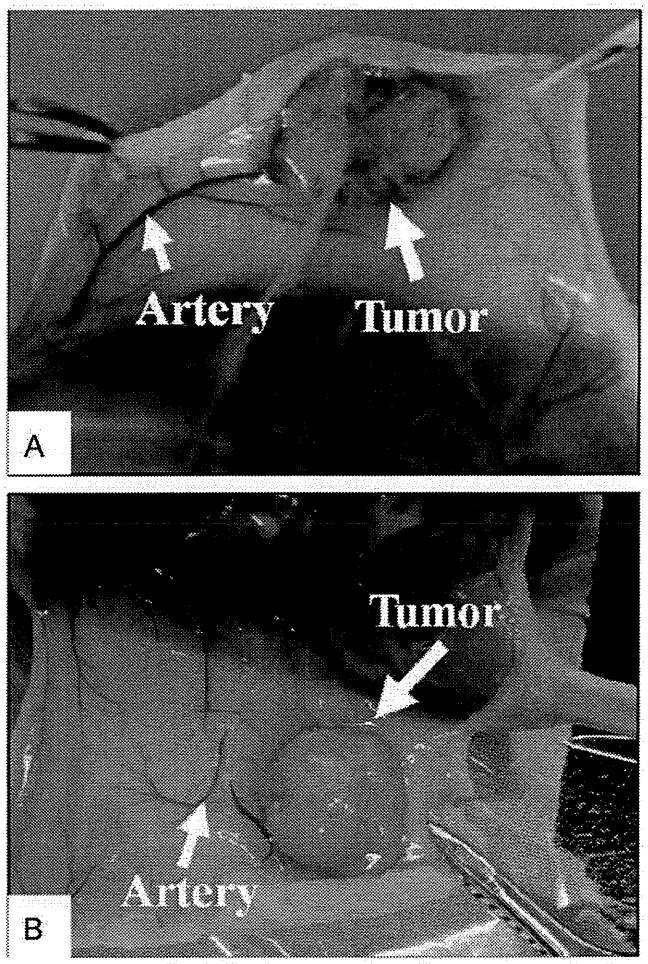

Fig. 2. Photographs showing CCS formation in dorsal region (A, Fujimoto et al., in press) and femoral region (B) of nude mice. Significant angiogenesis can be seen especially in the dorsal region.

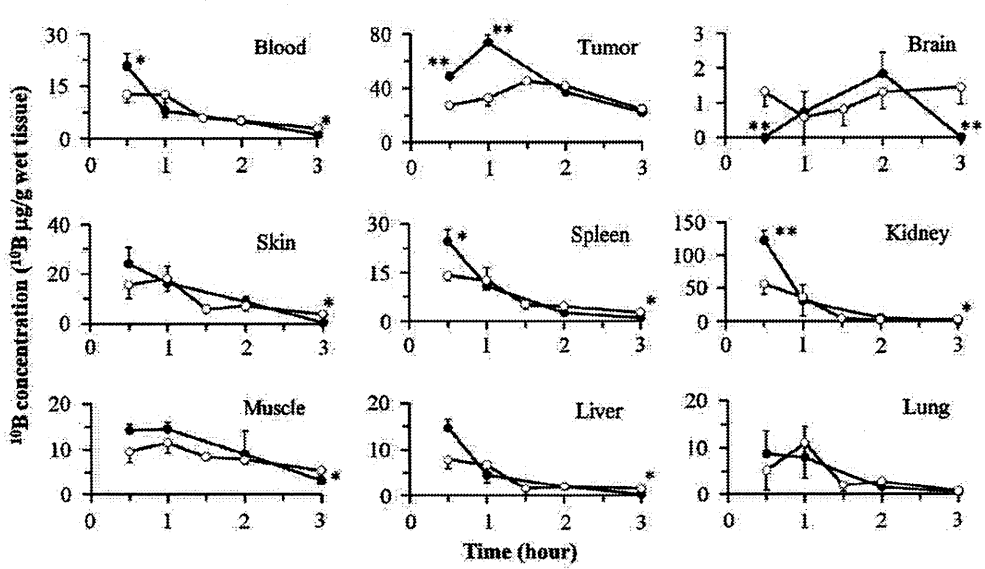

Fig. 1. Time course changes of ^{10}B concentration in tissues after i.v. administration of BPA-Fr (500 mg BPA/kg) to nude mice having MP-CCS-SY in dorsal region (●) and those in femoral region (○). *: $p<0.05$, **: $p<0.01$, significantly different from the ^{10}B concentration of dorsal region. Each value represents the mean ± S.D. ($n=3$).

femoral vein to each tumor-bearing nude mouse under anesthesia with diethyl ether. At predetermined time intervals after dosing, blood sample was collected by cardiac puncture under deep anesthesia and then residual blood in the organs was removed by saline perfusion. Subsequently, the nude mice were sacrificed with diethyl ether. Tissue samples including the liver, spleen, kidney, lung, brain and tumor were collected immediately, washed with saline and lightly blotted to remove any excess blood and water. The skin and muscle were collected from the nates of the mice. The liver, kidney, brain and tumor were homogenized by a high-speed homogenizer.

2.5. Histological evaluation

The tumor mass was resected from the dorsally MP-CCS-SY-bearing nude mouse sacrificed one hour after intravenous administration of BPA-Fr (500 mg BPA/kg) under anesthesia with diethyl ether. This mass was routinely processed by fixation in formalin for overnight at 20–23 °C and then embedded in paraffin. Serial tissue sections were cut from the paraffin block, placed on glass slides and dried overnight. A part of the sections was stained with hematoxylin–eosin (H.E.) according to standard protocols for histological examination. Separately, some of the sections were incubated with anti-BPA Mab, stained with LSAB2 kit/HRP (DAB) and then counterstained with hematoxylin by the procedure described in the literature (Nakagawa, 2006) to visualize microscopic distribution of L-BPA in the tumor tissues.

2.6. Determination of boron

Quantitative determination of boron was carried out by the inductively coupled plasma atomic emission spectrometric (ICP-AES) method. A weighed sample of tissues or homogenates (typically 100–200 mg) was hermetically digested with $HClO_4$ (0.6 mL) and H_2O_2 (1.2 mL) for 48 h at 75°C. The resulting solution was diluted with ultra pure water to be 5 mL in total volume, followed by filtration with a 0.45 μm disposable filter unit. Boron concentration in each sample was determined by ICP-AES (SPS 3100, SII NanoTechnology Inc., Tokyo, Japan). The emission intensity was measured at 249.773 nm. The calibration curve obtained from dilutes of the boron standard solution (1000 μg/mL) was linear in the range of 0.2–10 μg/mL.

3. Results and discussion

The biodistribution data of boron after i.v. administration of BPA-Fr (500 mg BPA/kg) are shown in Fig. 1. As a general tendency, the boron concentrations in blood, spleen, kidney, liver and skin decreased rapidly after i.v. administration of BPA-Fr. The peak boron concentrations did not exceed 25 μg ^{10}B/g in the liver, spleen, brain, lung, muscle and skin, while the transiently high boron concentration was found in kidney. In contrast, the boron concentration in tumor increased rapidly, peaked at 1 or 1.5 hours, and subsequently decayed with time. The peak concentration reached 74 μg ^{10}B/g wet tumor tissue (ppm) for dorsally tumor-bearing mice and 45 ppm for femorally tumor-bearing mice, respectively (Fig. 1). This concentration was higher than the minimum effective concentration of boron, i.e., 20–30 μg ^{10}B/g (Barth et al., 1992) in BNCT. Such a high boron concentration in the CCS-bearing animals would be attributable to a high cell-uptake and/or cell-affinity of L-BPA (Fujimoto et al., in press).

The dorsally tumor-bearing mice showed significantly higher peak boron concentrations in tumor, compared with the femorally tumor-bearing mice (Fig. 1). As represented in Fig. 2, the CCS in dorsal region resulted in somewhat more distinct angiogenesis than the CCS in femoral region. This difference in the extent of angiogenesis may account for the higher boron concentration in dorsally tumor-bearing mice.

Both tumor-to-blood (T/B) and tumor-to-skin (T/S) ratios should be large enough in order to avoid radiobiological damage to the normal skin. The T/B and T/S ratios at 1 hour after administration of BPA-Fr in dorsally tumor-bearing mice were 9.2 and 4.5, respectively, while those at 1.5 hour after administration of

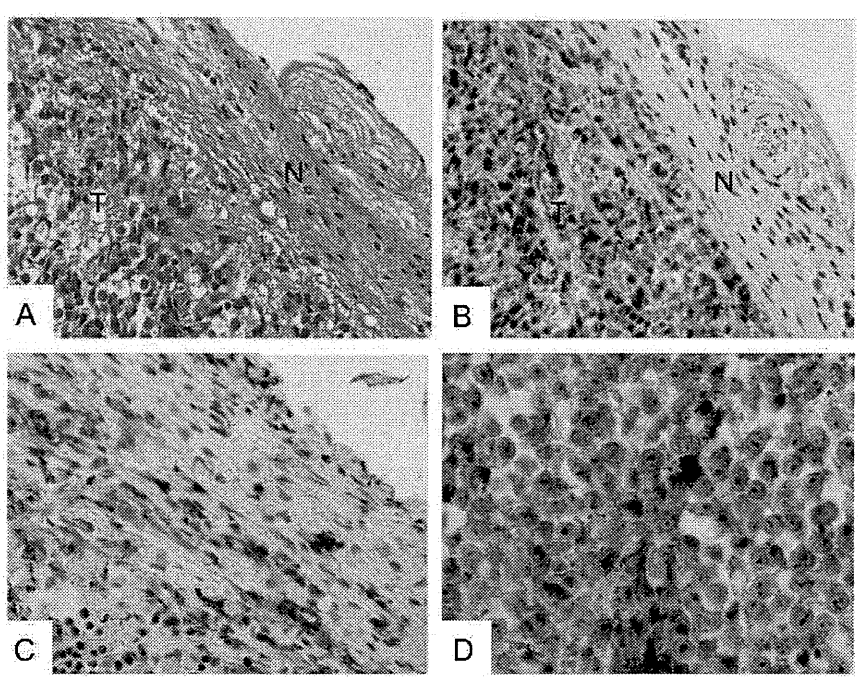

Fig. 3. Micrographs (100×) showing tumor sections (T) with the surrounding normal tissues (N) resected from BPA-administered mice (A, B, D) and non-BPA-administered mice (negative control, C). A: Hematoxylin-Eosin staining; B–D: immunostaining with anti-BPA MAb. D represents a magnified image (×400) of B.